

The Optical Telescope Project

Imaging Messier 42, Dimming of Betelgeuse, and Stellar Spectroscopy

Dhruv Gандотра

1708050

Third Year Project in Physics

Submitted to King's College London
Supervisor: Professor Malcolm Fairbairn

Department of Maths
Department of Physics

1st April, 2020

Abstract

In this report, we explained in depth the methods and experimental techniques we applied on the data collected using our university's optical telescope. This included capturing and manipulating images of the diffuse nebula, Messier 42, using an imaging software, GIMP. Additionally, our project luckily overlapped with the strange dimming of the star, *Betelgeuse*. We positively correlated its dimming and subsequent brightening an online tracking of its apparent magnitude by taking telescopic pictures of our own and running some codes on it with Python. However, due to the small dataset we were able to produce, and the wary external conditions in London, these deductions should be taken with a pinch of salt. Finally, out of curiosity, we also took spectral images of various stars of all different stellar types with a spectroscope and analysed the expected trends and characteristics of the spectral lines generated from their spectra, also using Python.

Contents

1	Introduction	1
1.1	Project Aims	1
1.2	Messier 42	1
1.3	Stellar Classification	1
1.4	Betelgeuse	3
1.4.1	Apparent and Absolute Magnitude	4
1.4.2	The Dimming of Betelgeuse	4
2	Methods	5
2.1	Experimental Equipment	5
2.2	Telescope Calibration and Alignment	6
2.3	M42 - Imaging and Image Manipulation	6
2.4	Betelgeuse and Bellatrix	6
2.4.1	Imaging	6
2.4.2	Coding	7
2.5	Spectroscopy	8
2.5.1	Imaging	8
2.5.2	Coding	8
3	Results	10
3.1	Messier 42	10
3.2	Betelgeuse	11
3.3	Stellar Spectra	13
4	Discussion	15
4.1	Limitations	15
4.2	Messier 42	16
4.3	Betelgeuse and Bellatrix	16
4.4	Stellar Spectra	17
5	Conclusion	17
6	Code	18
6.1	Sessions 1-5	18
6.2	Betelgeuse Tracking	21
6.3	Stellar Spectra	28
	References	31

1 Introduction

Astronomy meaning “law of the stars” is one of the oldest natural sciences. It dates all the way back to the earliest civilisations such as the Babylonians, Mayans, Egyptians, and many indigenous American tribes, among others. It is a field that started as an aid for crop growing, time and date keeping, navigation, and ceremonial uses. Now, it is serves more as a purpose to discover the beautiful and mysterious truths of the Universe. [1]

Today, astronomy is typically divided into two branches, observational and theoretical. Observational astronomy concentrates on gathering data from observations of celestial bodies, which is then interpreted using the laws of physics. Theoretical astronomy then aims to use these findings to explain theoretical predictions. The two branches go hand in hand. It is one of the few fields today that do not require you to be an academic. Anyone with a telescope and a curious mind can help progress this wonderful science.

1.1 Project Aims

There were three main aims of this project. Firstly, taking images of M42 using the telescope at our university and manipulating them in an image manipulation software called GIMP to produce a final coloured image. However, the focus of this report was the constellation of Orion, specifically Orion’s Nebula which contains the star *Betelgeuse*. Recently, the star underwent a sudden and drastic dimming phase. The motivation was to correlate this dimming with observations taken using the telescope and to analyse the severity of this dimming using computer coding and other telescopic readings. In addition, we looked at some spectral lines produced by taking pictures of stars from each spectral group (OBAFGKM) because we felt that these results would help our understanding of stars in general.

1.2 Messier 42

The Orion Nebula, or Messier 42, or M42 is part of the Orion Constellation. It is a component of Orion’s Sword alongside three stars, *42 Orionis*, *Theta Orionis*, and *Iota Orionis*. It has been a point of interest for many centuries due to its high brightness, and the fact that it visible to the naked eye. It is also at a distance of $1,344 \pm 20$ light years, making it the closest area of massive star formation to us. [2] Due to its proximity and visibility, M42 has helped us vastly in understating how clouds of gas and dust collapse to form stars and other planetary systems. For the same reasons, we picked M42 as a starting point to photograph and manipulate in GIMP, which also helped us familiarise with the program for coding purposes.

1.3 Stellar Classification

Stars are typically classified using their photosphere (star’s outer shell) temperatures, which in turn give information about their spectral characteristics. Their spectral absorption lines and their corresponding strengths tell us about what elements the stars are mainly comprised of, and their abundance. The main system of classification used is the Morgan-Keenan (MK) system described below, which uses the letters O (hottest), B, A, F, G, K, and M (coolest). [3]

- O-type: Extremely hot and luminous, blue stars with surface temperatures exceeding 30,000 K, main sequence star masses being at least $16 M_{\odot}$ (solar mass), and main sequence star radii greater than $6.6 R_{\odot}$ (solar radius). Strong He I (neutral He) and He II (ionised He) spectral lines, along with faint H lines. Also, have prominent ionised (Si IV, O III, N III, and C III) lines. Rarest type of main sequence stars, only 1 in 3,000,000 (0.00003%) main-sequence stars being O-type.

- B-type: Very hot and luminous, blue-white stars with temperatures anywhere between 10,000 and 30,000 K, masses between $2.1\text{-}16 M_{\odot}$, and radii between $1.8\text{-}6.6 R_{\odot}$. Present are prominent He I, He II, and Si II lines with moderate H lines. Around 1 in 800 (0.125%) stars are B-type.
- A-type: Relatively warm and luminous, white stars with temperatures between 7,500 and 10,000 K, masses between $1.4\text{-}2.1 M_{\odot}$, and radii between $1.4\text{-}1.8 R_{\odot}$. Strongest H lines, along with some lines of ionised metals (Fe II, Mg II, Si II). This is also where the Ca II lines start to appear. Roughly 1 in 160 (0.625%) stars are A-type.
- F-type: These stars are white in colour with temperatures ranging between 6,000 and 7,500 K, masses between $1.04\text{-}1.4 M_{\odot}$, and radii between $1.15\text{-}1.4 R_{\odot}$. Slightly weaker H lines than A-type stars with similar lines of ionised metals. Ca II lines getting stronger. About 1 in 33 (3.03%) stars are F-type.
- G-type: This category includes the Sun and these stars are yellow in colour. Temperatures are anywhere between 5,200 and 6,000 K, masses are between $0.8\text{-}1.04 M_{\odot}$, and radii are between $0.96\text{-}1.15 R_{\odot}$. Strongest Ca II lines with even weaker H lines than F-type stars. They also have ionised metal lines along with neutral metal ones. Around 1 in 13 (7.7%) stars are G-type.
- K-type: These stars are light orange and lower in temperature, between 3,700 and 5,200 K. Their masses are between $0.45\text{-}0.8 M_{\odot}$, and radii are between $0.7\text{-}0.96 R_{\odot}$. Extremely weak H lines, if any. Strong lines of neutral metals (Mn I, Fe I, Si I). Titanium Oxide (TiO) lines starting to appear as well. About 1 in 8 (12.5%) stars are B-type.
- M-type: The coolest and dimmest of them all, these orange red stars have temperatures ranging 2,400 to 3,700 K, masses between $0.08\text{-}0.45 M_{\odot}$, and radii less than $0.7 R_{\odot}$. They cannot be seen with the naked eye due to their extremely low luminosities. Lines of oxide molecule are visible, especially TiO, along with other neutral metals. Vanadium(II) Oxide lines start to appear also. They are by far the most common type with 76% of stars being M-type.

Each letter is then subdivided using the numbers 0 (hottest) to 9 (coolest). The MK system also adds a Roman numeral, used to denote the star's luminosity class. A Hertzsprung-Russell (H-R) diagram is often used to accurately describe the MK classification system, and its respective subcategories.

- 0 or Ia+ - Hypergiants
- Ia - Very luminous Supergiants
- Ib - Less luminous Supergiants
- II - Bright Giants
- III - Normal Giants
- IV - Subgiants
- V - Main Sequence Stars (Dwarfs)
- VI - Subdwarfs
- VII - White Dwarfs

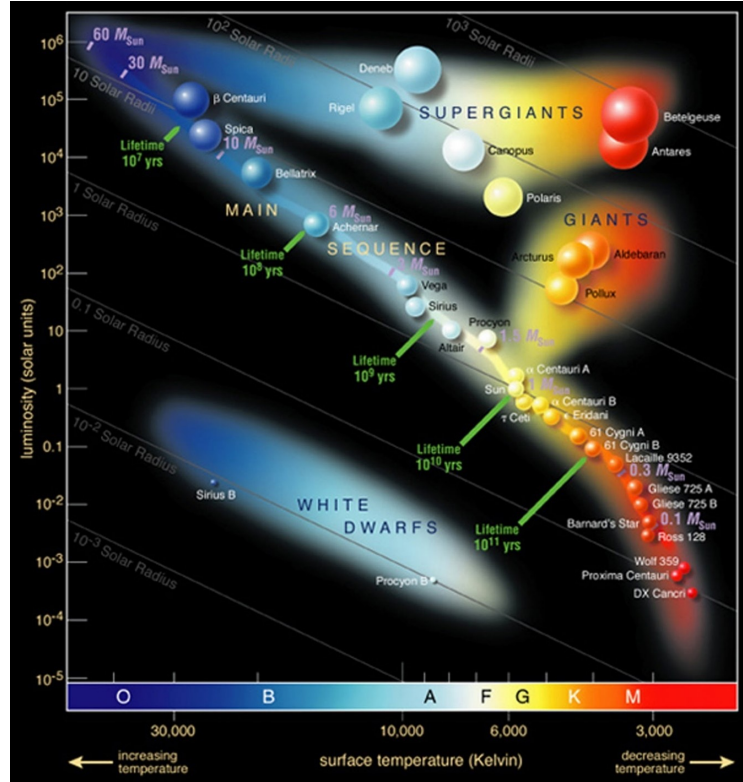


Figure 1: H-R diagram along with luminosity, surface temperature, and some examples.

1.4 Betelgeuse

Betelgeuse, also known as *Alpha Orionis*, is the second brightest star in the Orion constellation behind *Rigel*, making it easily visible to the naked eye. It is situated on the right shoulder of the Orion. The name, *Betelgeuse*, comes from the Arabic phrase *Ibt al-Jauza*, meaning the “Armpit of Orion”. It is a reddish supergiant with a mass 9.5-21 times that of the sun, and its radius is about 1,000 times of the sun. However, it is calculated to have started its life at about $15-20 M_{\odot}$. Since 1993, the star is continually losing mass, about $1 M_{\odot}$ every 10,000 years, causing it to be engulfed by a sort of nebulae around 250 times bigger than *Betelgeuse* itself.

Some parts of the mass have been blown off into space by very powerful solar winds, reaching up to more than 30,000 AU (approximately the distance from Earth to the sun) away from the star. In fact, it is so massive that if it replaced our sun, it would extend past Jupiter’s orbit. It has a rotation and revolution period of roughly 400 days and 15-30 years respectively, and it travels at around 30 kmph. Its distance to us being around 700 lightyears (200 parsecs). It is classified as a M-type star (M1-2Iab) that is believed to have evolved from an O-type star, and its apparent magnitude varies between 0.3 and +1.2. [4]

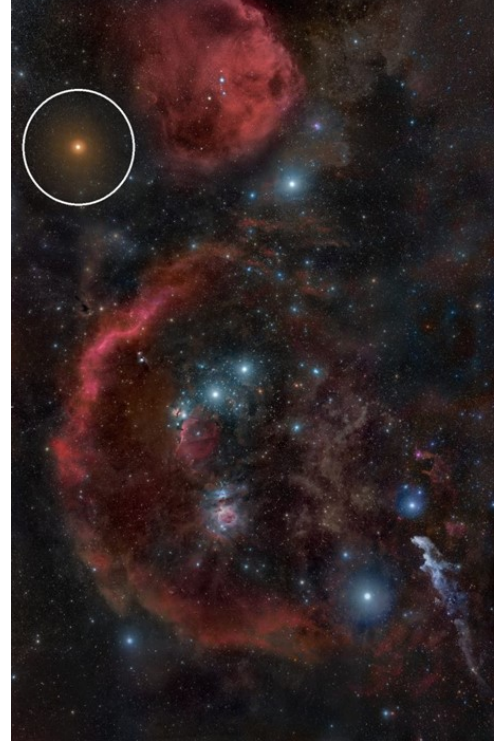


Figure 2: Picture of the Orion constellation, taken by Rogelio Bernal Andreo in October 2010. *Betelgeuse* is circled in the top left.

1.4.1 Apparent and Absolute Magnitude

This is a tool used by astronomers to determine the brightness of a celestial object, and depends on the body's intrinsic luminosity, its distance from Earth, and any extinction (absorption or scattering of electromagnetic radiation due to interstellar dust or gas) of the object in the field of view of the telescope. To be precise, brightness implies the flux of light in W/m^2 . The scale is reverse logarithmic, meaning the brighter the body, the lower its apparent magnitude. How the scale works is if an object is 5 magnitudes higher than another, it is 100 times dimmer. Therefore, if the difference is 1.0 magnitude, the brightness ratio is $\sqrt[5]{100}$, roughly 2.512 (Pogson's ratio). The point of zero magnitude is taken as the brightness of *Vega*, whilst the apparent magnitude of the sun is -26.74, making it the brightest object visible from Earth. The maximum magnitude (dimmest star) visible to the average naked eye is about +6.5, under great conditions.

Another measurement widely used is absolute magnitude. It is defined as the object's apparent magnitude if it was viewed from a distance of exactly 10 parsecs (32.6 light years). [5] Currently, the highest observed absolute magnitude is -14.2, of the star LBV 1806-20, making it at least 5,000,000 times brighter than our Sun. While, the dimmest star observed is a white dwarf in the NGC 6397 cluster, with an absolute magnitude of around +28. This star is so dim that its brightness is comparable to that of a birthday candle on the Moon, viewed from Earth. [6]

$$m_x = -2.5 \log_{10} \left(\frac{F_x}{F_{x,0}} \right) \quad (1)$$

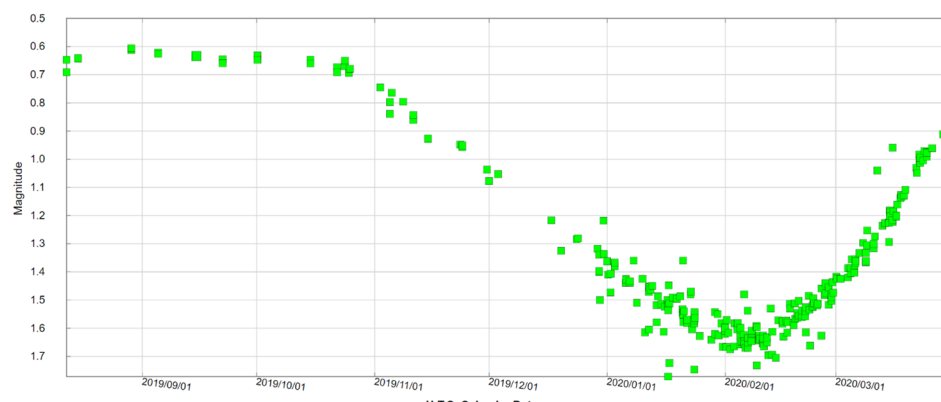
Equation (1) shows how to calculate the apparent magnitude in the spectral filter x (m_x), where F_x is the observed flux density in that spectral filter and $F_{x,0}$ is the zero point of that filter.

$$M = m - 5 \log_{10} (d_{pc}) + 5 \quad (2)$$

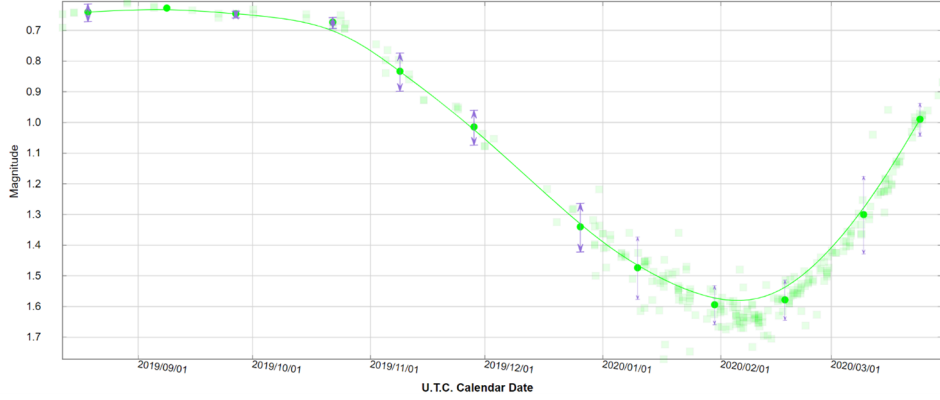
Equation (2) shows how to convert apparent magnitude (m), to absolute magnitude (M), using the distance from the object to the observer in parsecs (d_{pc}).

1.4.2 The Dimming of Betelgeuse

Betelgeuse is a semiregular pulsating variable star (giant or supergiant showing periodicity in light changes), making it very unpredictable. It has an apparent magnitude of around +0.5. However, in November of 2019, it went through a drastic dimming phase, to an apparent magnitude of around +1.5 by January of 2020. This meant that the star's brightness had reduced by roughly 2.5 times. [7]



(a) Apparent magnitude of *Betelgeuse*



(b) Mean apparent magnitude of *Betelgeuse* with a line of best fit

Figure 3: Graphs showing the decline in apparent magnitude of *Betelgeuse* in the V-band between 01/07/2019 and 31/03/2020. Apparent magnitude is represented on the inverse y-axis, and the dates are plotted on the x-axis in the format yyyy/mm/dd. (a) The raw data is shown by the green squares. (b) The mean data points are represented by the solid green circles along with error bars. A line of best fit with a bin size of 20 days is also included for a clearer interpretation. All data and graphs were produced from the American Association of Variable Star Observers.

This unexpected dimming caused a lot of intrigue amongst the scientific community. Many online articles were published by the media, falsely predicting a supernova in the near future. Considering a star of this mass, the end of its life cycle will definitely cause a supernova, but the chances of it randomly exploding in our lifetime is less than 0.1 %. So, the better question is when will *Betelgeuse* supernova and what will it leave behind? The combination of its size and temperate tells us that it will probably explode in the next 10,000 to 100,000 years, probably leaving behind a neutron star. However, if its mass is closer to its upper limit, the remnant of the explosion could even be a black hole. [8]

2 Methods

2.1 Experimental Equipment

- Telescope Model - Celestron EdgeHD 14 Inch Optical Tube Assembly
- Guide Telescope - Celestron Guide Scope
- Camera Model - Atik 383L+
 - Filter 1: 410-500 nm
 - Filter 2: Hydrogen alpha (H α) - 656 nm
 - Filter 3: Oxygen-III (O III) - 496 and 501 nm
 - Filter 4: Sulphur-II (S II) - 672 nm
 - Filter 5: Green - 500-550 nm
- Spectrometer Model - Baader Dados
- Camera computer software - Artemis
- Telescope tracking software - PhD Guiding 2

2.2 Telescope Calibration and Alignment

Every session, before taking any pictures using the telescope, the eyepiece cross hairs on the telescope needed to be aligned. Firstly, the telescope was aimed at the Centre Point building near Tottenham Court Tube Station (roughly 1km away). After part of the lit “Centre Point” on top of the building was in the centre of the computer’s screen, the eyepiece was tweaked such that the cross hairs were aimed at the centre of what the screen was showing.

Once the eyepiece cross hairs were calibrated, the telescope was aligned. This was achieved by entering the then date and time into the telescope’s control panel, before selecting the previous alignment. Once we aligned the telescope manually, by using a two-star alignment (*Sirius* and *Capella*) with an additional calibration star (*Regulus*). For each star, the telescope pointed and was then adjusted so that the star was at the centre of the screen. As previously mentioned, the eyepiece was then corrected to make the cross hairs point at the centre of the star. The alignment was complete, and the telescope could then be used to look at an object of interest.

2.3 M42 - Imaging and Image Manipulation

We took two sets of images of M42, first with 20s exposure and 1x1 binning. Five images per filter were taken with the purpose of reducing noise by averaging. Then, we opened these images in the image processing software GIMP, as layers, one filter at a time. We chose one of the images as our base image, and then proceeded to align the remaining four images with the base image, individually. This was achieved by overlapping the images, as we best as we could, using the rotation and move tools. The five aligned images were then merged to produce a single image. This process was repeated for all five filters resulting in one image per filter. Unfortunately, the images of filters 1 and 5 were overexposed, and were therefore removed. Lastly, we used the colour balance tool and assigned a colour each to filters 2,3,4 and merged the three stacked images to produce one final image.

The second set of images were taken with 120s exposure and 2x2 binning instead, but using only filters 2,3,4 (due to the reason mentioned above). The higher exposure and binning were made possible thanks to the auto tracking technology; designed to keep the telescope fixed on our target. As before, the images were manipulated in GIMP, resulting in another final image. Sadly, the auto tracking software was erratic and unsteady, making this the only time we could use it. Both final images are compared in the results section

2.4 Betelgeuse and Bellatrix

2.4.1 Imaging

After taking images of M42, we proceeded to take images of *Betelgeuse* and *Bellatrix* to determine the trend in the brightness of *Betelgeuse*. *Bellatrix* was taken as a reference point as it was relatively constant, and it also helped us eliminate the photographic noise every night. All these images were taken with filter 2, using 1x1 binning. The exposure time was initially 0.2s but was then reduced to 0.1s after the first session, to prevent overexposure. This was done by adjusting the exposure time to make sure the brightest pixel had a value less than 65536 (256x256). In addition, every night before the images were captured, we zoomed in on the star in question using the computer, to get a better view of it. We took around 10-20 images of each star each session. This time however, these images were stacked using Python, instead of GIMP.

2.4.2 Coding

These sets of images were merged in Python for various reasons. Firstly, it was much harder to align 10-20 images manually in GIMP. Secondly, most of the images were pre-aligned. Any unaligned images were removed from the code, although they were very few of them. Lastly, we are interested in the value of the pixels this time, rather than their position. Also, all the codes are shown in the code section

After opening the *Betelgeuse* images of that session in Python, they were converted to arrays and each element was divided by 256 to make the pixel values more manageable, as each pixel value was between 0 and 65536. The average of all the arrays was calculated and plotted. The plot was then converted back into a picture and a 50x50 pixel cut out was taken around the star itself to reduce any hot pixels, ice crystals or background noise that may have appeared. Finally, the cut out was then converted to an array. The sum of the elements of the resulting array was calculated, while the array was represented as graph to visualise the pixel values. For us, that sum represents the brightness of the star.

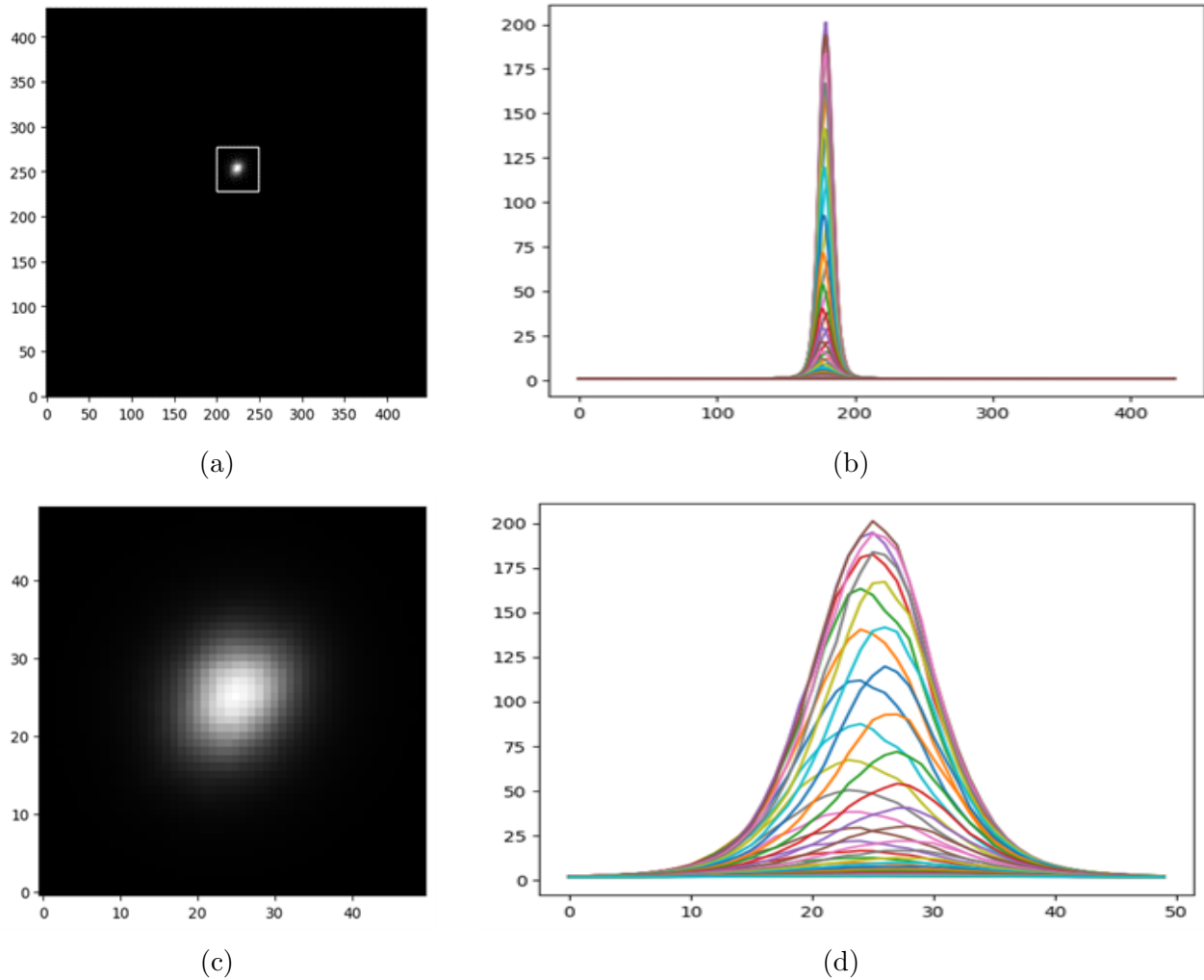


Figure 4: (a) 14 stacked images of *Betelgeuse* from Session 1 - 28/01/2020. The x and y axes represent pixel coordinates. (b) Plot of 2-D array of image in a. The x and y axes represent pixel row and brightness, respectively. Each coloured line represents a column of pixels, with each pixel having a brightness value ranging between 0 and 256. (c) 50x50 pixel cut out of stacked image in Figure 4a. (d) Cropped image in Figure 4c, converted to a 2-D array and plotted. Each coloured line represents a column of pixels, with each pixel having a brightness value between 0 and 256. Essentially, a crop of Figure 4b.

The same procedure was repeated for all the *Bellatrix* images of that night. Lastly, the experimental difference in apparent magnitude between *Betelgeuse* and *Bellatrix* was calculated after each of the five different sessions using Equation (3) and analysed in another code.

$$m_2 - m_1 = 2.5 \log_{10} \left(\frac{b_1}{b_2} \right) \quad (3)$$

Equation (3) shows the relationship between the apparent magnitudes of two stars (m_1 and m_2), and their brightness (b_1 and b_2).

2.5 Spectroscopy

Spectroscopy involves imaging objects with a spectrometer and analysing the absorption and emission lines produced, known as spectral lines. These lines are due to outer shell electrons being electronically transitioned from one electron orbit to another. The atoms absorb energy if the electron jumps to a higher energy level and emit energy if it moves to a lower energy level; both in the form of photons. The wavelength of these lines and how strong they are, correspond to the identity and concentration of the elements they are made of. We compared spectra of stars from different spectral groups to see what elements are found in what types.

2.5.1 Imaging

Taking pictures for stellar spectra involved the same set up; however, the Atik 383L+ camera was now replaced with the Baader Dados spectrometer. The equipment required a lot of precision because the apparatus was very sensitive. We recorded data of stars from each spectral class so we could have a complete range of spectra.

- O-type: *Alnitak*
- B-type: *Alnilam*, *Regulus*
- A-type: *Alhena*, *Sirius*
- F-type: *Procyon*
- G-type: *Capella*
- K-type: *Alphard*
- M-type: *Betelgeuse*

2.5.2 Coding

The coding for spectral analysis was much easier because it used a code very similar to the *Betelgeuse* and *Bellatrix* code. As before, the image for each star was loaded up. The image was then cropped using a cut out that spanned the width of the image (1677 px) and with a height enough to capture the whole spectra (150 px), as it was not perfectly horizontal. The cropped image was then converted to a 2-D array and integrated over the columns to get the spectral lines. The array was then plotted. If there were two images of the star, both images went through the same process, and a mean was calculated and used instead. The problem we now faced was that the x-axis was in pixel columns which did not convey any information. To counter this, we found the pixel column associated with as many prominent troughs as possible by finding the local minimum using trial and error.

After some online research, corresponding wavelengths of elements (\AA) were found for the troughs by using the spectral type of the star we were looking at. The pixel column and the associated wavelengths were then plotted on the x and y axes, respectively, giving us a line of best fit and its equation. We used that equation to scale the pixel columns to wavelength instead and plotted our final spectrum with the corresponding elemental lines marked and labelled. Finally, we found that pictures were actually increasing in brightness from left to right. To achieve uniformity, the black-body spectrum is usually used to normalise the spectrum, but we could not manage to generate it in time. Instead, we drew a rough polynomial fit, with 4 being the best degree, and normalised the spectrum. This was done by dividing the original stellar spectrum with the polynomial curve. Eventually, this whole process was repeated for every star in every spectra type and compared. Here is *Sirius* as an example.

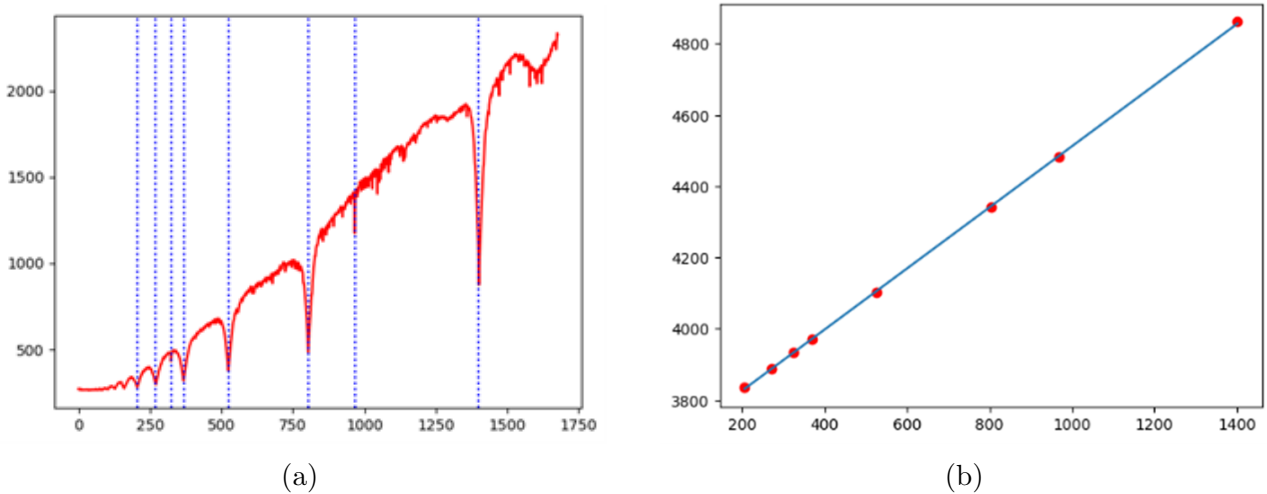


Figure 5: (a) Stellar spectra of *Sirius* before scaling. The troughs represent absorption at specific wavelengths. (b) Plot of pixel columns from a on the x-axis, and the corresponding wavelengths (\AA) found online on the y-axis.

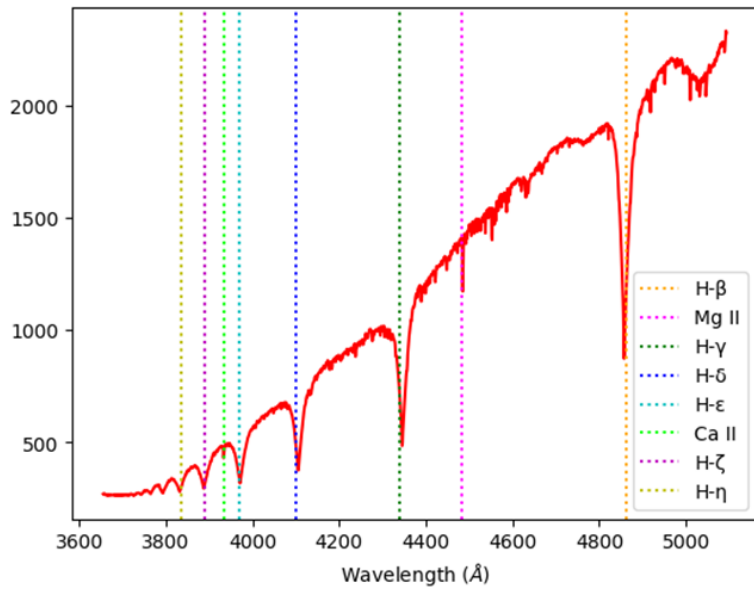


Figure 6: Final absorption spectrum of *Sirius*. Wavelength on the x-axis is scaled from pixel column to angstroms (\AA) using the equation of the line of best fit in Figure 5b. Also shown are marked and labelled spectral lines with their associated elements.

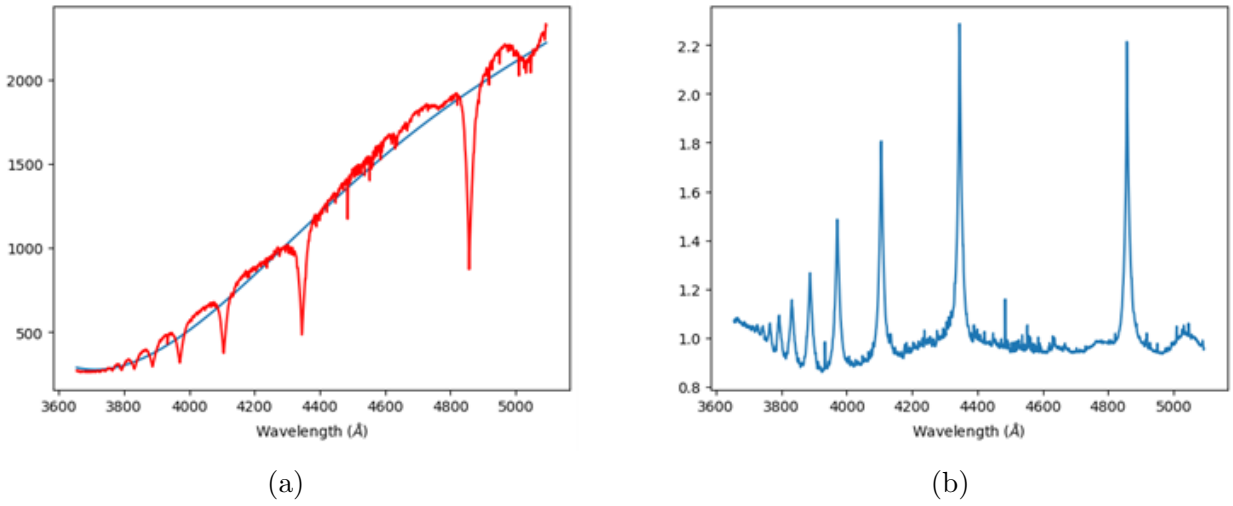


Figure 7: (a) Final spectrum of *Sirius* with a polynomial fit of degree 4. (b) Normalised *Sirius* spectrum using the polynomial fit in a.

3 Results

3.1 Messier 42

The first task involved us taking pictures of M42 using our telescope. After playing around with exposure times and binning, we finally decided on 20s exposure and 1x1 binning for the best results. Following manipulation in GIMP, the final image is displayed in Figure 8a. Even though we only managed to get the auto tracking to work once, it produced some high-quality images at 120s exposure and 2x2 binning, shown in Figure 8b. You can clearly see the difference in resolution due to the added help.

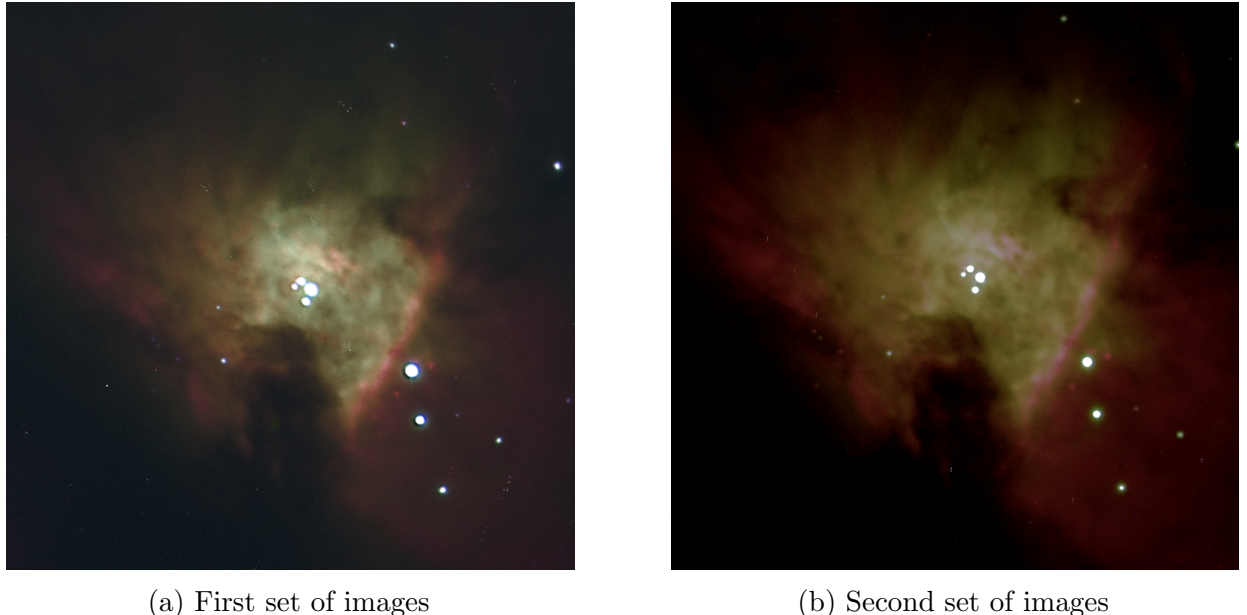


Figure 8: Final stacked images of Messier 42. Both images are a combination of images taken with filters 2,3,4 (H α , O III, and S II respectively), and false colour is also added to each filter. In this case, red, green, and blue. (a) Result of images taken with 20s exposure and 1x1 binning. (b) Result of images taken with the aid of the Celestron Guide scope and the PhD Guiding 2 software, using 120s exposure and 2x2 binning.

3.2 Betelgeuse

The purpose of our code was to find a trend in the apparent magnitude of *Betelgeuse*. This was achieved using the sum of the averaged arrays of the images of *Betelgeuse* of *Bellatrix* on each night and finding the image brightness ratio. These ratios were then converted to values for the difference in apparent magnitude using Equation (3). Assuming that the apparent magnitude of *Bellatrix* is relatively constant each night, this would in theory, give us an indication of how *Betelgeuse*'s apparent magnitude is changing in this time period. Table 1 displays our values for the five sessions. All calculations were done in Python and shown in the Code section.

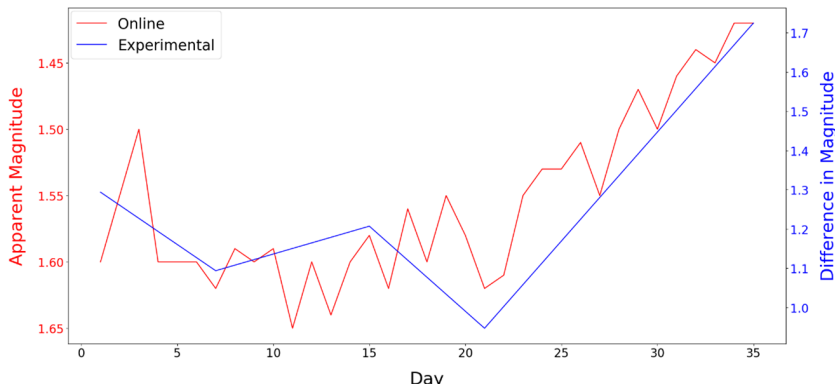
Date	Star	Total Image Brightness	Image Brightness Ratio	Apparent Magnitude Difference
28/01/2020	Betelgeuse	37,790.5	3.293	1.294
	Bellatrix	1,475.4		
03/02/2020	Betelgeuse	24,964.3	2.739	1.094
	Bellatrix	9113.9		
11/02/2020	Betelgeuse	17,577.9	3.041	1.207
	Bellatrix	5,780.9		
17/02/2020	Betelgeuse	14,992.6	2.393	0.948
	Bellatrix	6,264.0		
02/03/2020	Betelgeuse	19,119.1	4.896	1.724
	Bellatrix	3,905.3		

Table 1: Table of results comparing the total image brightness, image brightness ratio and difference in apparent magnitude between *Betelgeuse* and *Bellatrix* for the 5 sessions.

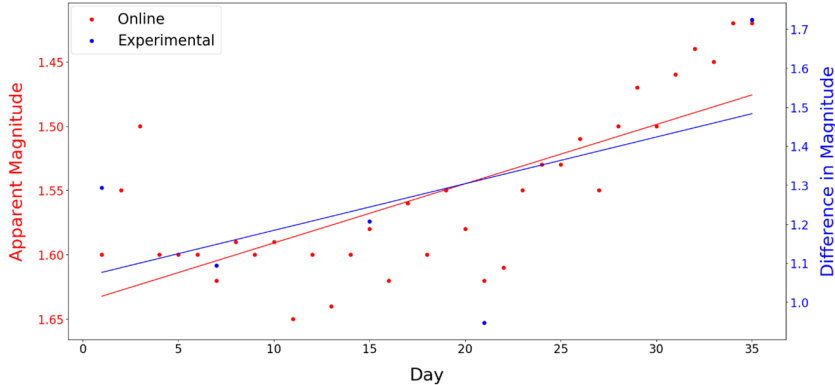
In another code, we compiled a list of values of apparent magnitudes of *Betelgeuse* from AAVSO observers. We generated a graph with the time period being all the way from 15/01 up until this report is written. Then, replaced the dates with number of days (for easier manipulation), and plotted a line of best fit and a polynomial fit, using Equation (4).

$$A_{k,j} = \sum_{i=0}^n x_i^{j+k}; b_k = \sum_{i=0}^n x_i^k y_i \quad (4)$$

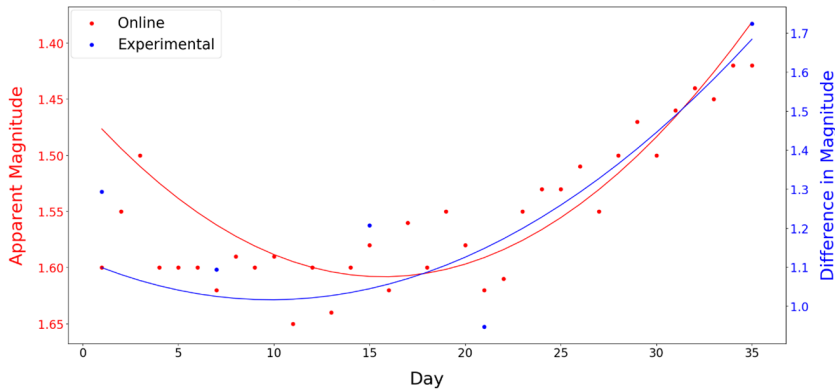
However, our last viewing session was on 02/03 so, we cropped the data to a period of 35 days, from our first session (28/01) to our last (02/03). This was done for a better comparison of our data with the reference data. After assigning the corresponding day number to our session dates (1,7,15,21,35), we produced three different graphs linking the trends in apparent magnitude side by side with the same x-axis, as shown in Figure 9.



(a) Comparison of raw online and experimental data



(b) Linear comparison of data using lines of best fit



(c) Polynomial comparison of data using polynomial interpolation

Figure 9: Comparison of *Betelgeuse*'s apparent magnitude values gathered by AAVSO and our experimental calculations in the difference in apparent magnitude between *Betelgeuse* and *Bellatrix*. The data ranges from days 1-35 (28/01/2020 - 02/03/2020).

The y-axis of the online data is inverted because *Betelgeuse* getting brighter corresponds to a decrease in apparent magnitude, but an increase in the apparent magnitude difference with *Bellatrix*; *Betelgeuse* having a lower magnitude than *Bellatrix*. Keep in mind, that we can only compare trends rather than the raw numbers because our code does not actually calculate the apparent magnitude of *Betelgeuse*, but instead calculates the apparent magnitude difference. This is because we do not have the necessary information needed shown in Equation (1). It is easy to see from the graphs in Figure 9 that the trends are highly similar. This is further correlated by the line of best fits in 9b and the polynomial fits in 9c matching up quite nicely.

- Gradient of online data linear fit: -0.0046
- Gradient of experimental data linear fit: 0.0120

Considering the inversion of the y-axis of the online data, we can ignore the negative sign of the online gradient, making the gradient values even closer to each other. The graphs also show that around day 22 (18/02), *Betelgeuse* started to brighten up again. The fact that the linear fit gradients are so close to 0 and the concave up nature of the polynomial fit further prove this projection. We should not get ahead of ourselves as we could only generate five data points; however, it is encouraging to see this level of agreement of a very small set data set with a much larger, more accurate data set. As a side note, here is the expanded version of the online data that better correlates the variability in *Betelgeuse*'s luminosity.

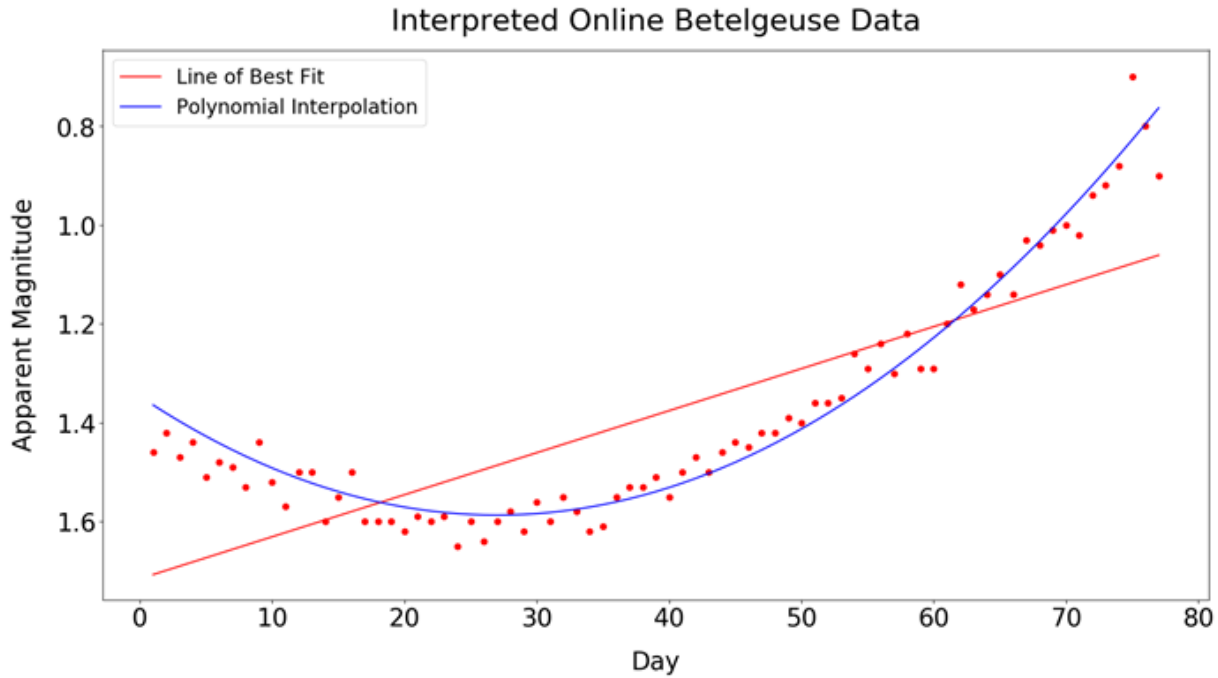
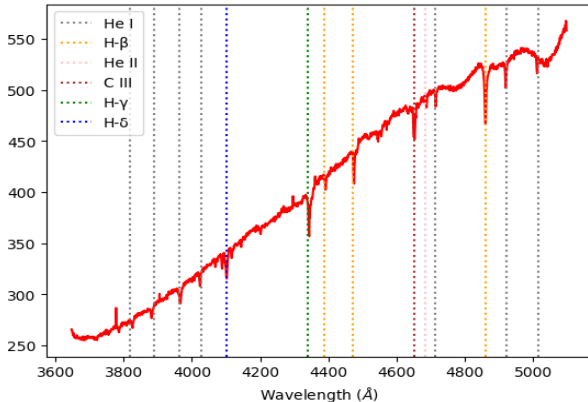


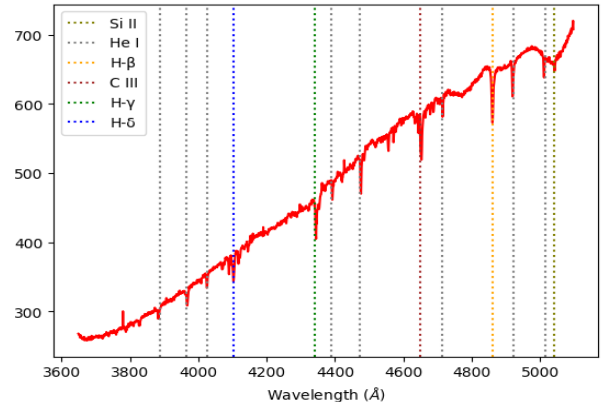
Figure 10: Complete graph of the collected data over 77 days. 15/01/2020 - 31/03/2020. A line of best fit and a polynomial fit is included for a clearer interpretation.

3.3 Stellar Spectra

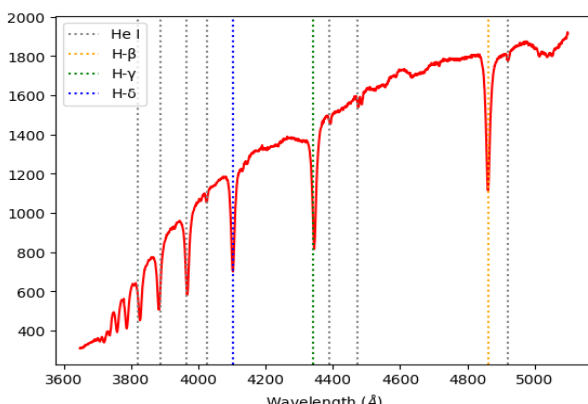
As mentioned previously, here are all the spectra that we produced in Figure 11.



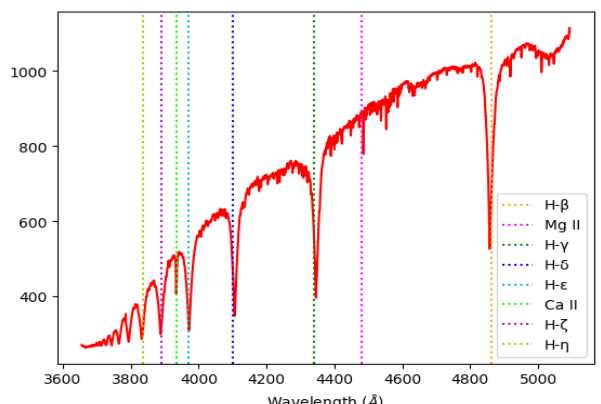
(a) Absorption spectrum of *Alnitak* (O)



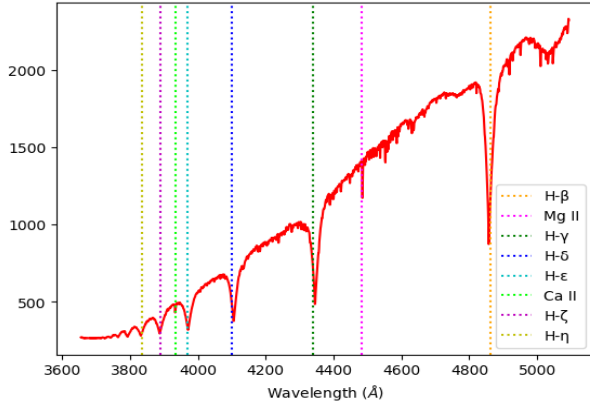
(b) Absorption spectrum of *Alnilam* (B)



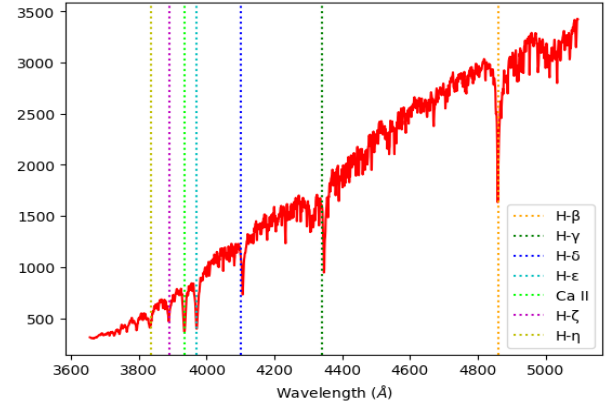
(c) Absorption spectrum of *Regulus* (B)



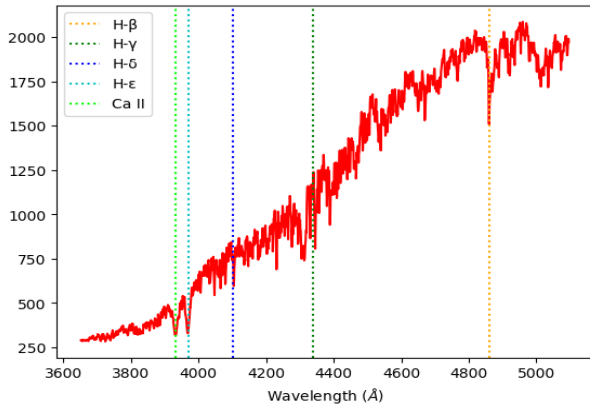
(d) Absorption spectrum of *Alhena* (A)



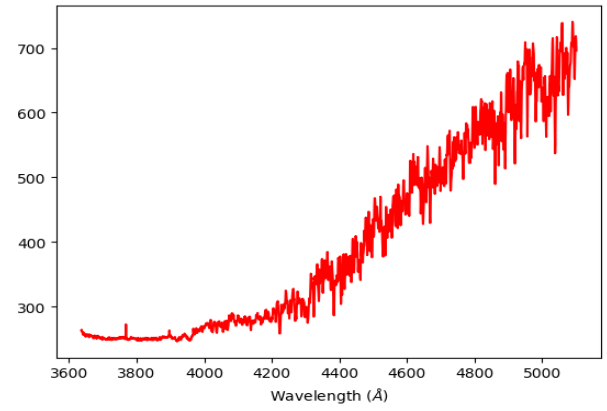
(e) Absorption spectrum of *Sirius* (A)



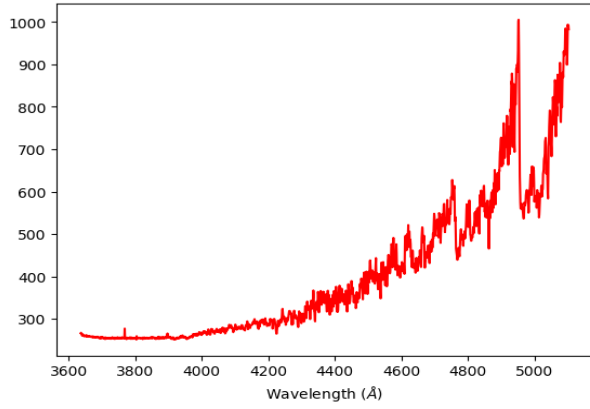
(f) Absorption spectrum of *Procyon* (F)



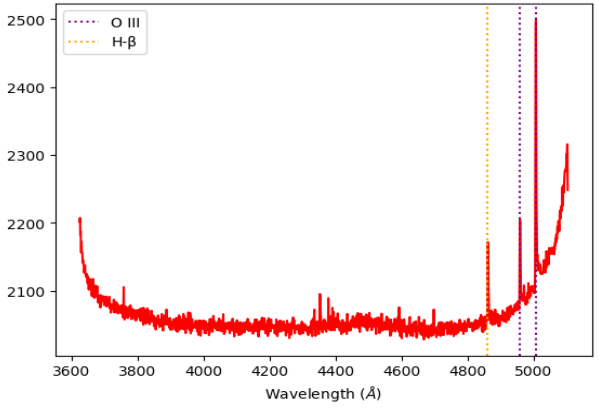
(g) Absorption spectrum of *Capella* (G)



(h) Absorption spectrum of *Alphard* (K)



(i) Absorption spectrum of *Betelgeuse* (M)



(j) Emission spectrum of *Messier 42*

Figure 11: Absorption spectra of 9 stars from different spectral types, and the emission spectrum of Messier 42 at 60s exposure. The x-axis represents wavelength (Å), and the spectral class of each star is also indicated in brackets.

Firstly, the last spectrum in Figure 11 is the emission spectrum of Messier 42, not an absorption spectrum. Absorption spectra are generated by stars because they have a core that excites electrons to higher energy levels by absorbing energy in the form of photons, producing absorption lines. However, electrons in nebulae lose energy over time because there is no energy source; causing the electrons to fall back to a lower energy level, and emitting photons; therefore, producing emission lines. Also, their spectra do not follow a black-body spectrum. The prominent emission lines seen in Figure 11j match really well with known wavelengths in the M42 spectrum, specifically H β ($\approx 4861 \text{ \AA}$), and two O III peaks ($\approx 4959 \text{ \AA}$ and 5007 \AA).

On the other hand, absorption spectra of stars follow a standard black-body curve with troughs corresponding to the absorption of photons by electrons of different elements with certain wavelengths. Although, we could only record part of the complete spectrum, roughly the first 1500 Å (blue and violet).

Additionally, the six Hydrogen lines seen across the various spectra are part of a set of seven, collectively called the Balmer series ($H\alpha$, $H\beta$, $H\gamma$, $H\delta$, $H\epsilon$, $H\zeta$, $H\eta$). We never captured $H\alpha$ because it has a wavelength of roughly 6565 Å, making it part of the red section of the visible spectrum and out of our possible range; while, $H\zeta$ and $H\eta$ are actually part of the ultraviolet spectrum. The Balmer series is an important part of stellar spectroscopy because it gives us an indication of the size and temperature of the star, and is often used as an identification marker for the stellar classification of stars.

Alnitak's spectrum also matches up nicely with the online values of multiple He I, along with He II and C III lines. Three H lines can also be seen, but they are quite faint because it is classified as a O9.51ab star (supergiant), and H lines weaken as an O-type star gets bigger.

As we move down the B-type subclasses, H lines get stronger, while He I lines get weaker. Therefore, it makes sense that *Regulus* has stronger H lines and weaker He lines than *Alnilam* because *Regulus* is classified as a B7V star (closer to A-type), and *Alnilam* is classified as a B01a star (closer to O-type). This is further proven by how similar *Alnitak* and *Alnilam*'s, and *Regulus*'s and *Alhena*'s spectra are. Another evidence of this is that like *Alnitak*, *Alnilam* also has a C III line, in addition to having a Si II line.

A-type stars are defined by their strong H lines, which are most pronounced at A0. They also display lines of ionised metals, namely Mg II and Ca II. Luckily for us, our A-type stars have the most prominent H lines, with *Alhena*'s lines (A0IV) being stronger than *Sirius*'s (A1V). Also, they both also display all six H lines within our wavelength range and have both ionised metal lines.

The features of F-type stars include weaker overall H lines and a stronger Ca II line than A-type stars. Both these features are correlated by comparing our *Procyon* (F5IV) spectra to *Alhena*'s and *Sirius*'s.

G-type stars have a very prominent Ca II, with the maximum at G2. The trend of H also continues with G-types having fainter H lines than F-types. Our *Capella* (G3III) spectrum confirms the change in H lines by having only four weak H lines, but for some reason has a weaker Ca II line than *Sirius*. However, this could be due to having a relatively noisy spectrum.

Unfortunately, our spectra of *Alphard* (K3III) and *Betelgeuse* (M1-21ab) were even worse. They were not clean enough to learn any info. Usually, spectra normalisation is a useful tool to help identify spectral lines, but even that proved futile here. [9][10][11][12]

4 Discussion

4.1 Limitations

Up until the 18th century, London was a rewarding place to be an astronomer in. It was home to the influential Royal Observatory in Greenwich, and the esteemed Royal Astronomy Society, the institutional home of this science. A lot of important astronomical discoveries were made here; however, by the end of the 1800s, it arguably became the toughest environment for astronomy. Even though The Industrial Revolution was pivotal in the advancement of technology, and in making Great Britain the superpower it is today, it has brought along with it a seemingly permanent and all-encompassing layer of light and air pollution that has only grown in area and strength over time.

The kind of light pollution we had to deal with is called sky-glow. It is defined as the orange glow above the horizon caused by the scattering of light in the atmosphere due to the high usage of artificial lights at night. It reduces the contrast between the sky and celestial bodies, making it harder to observe dimmer stars. Light pollution makes it more problematic to see diffuse sky objects like nebulae and galaxies because of their low surface brightness. Another issue is caused by air pollution and clouds, which reduce the intensity of photons from space captured by the telescope. This is due to the absorption and back-scattering of the cosmic radiation by the muggy atmosphere. [13]

Unfortunately, our limitations do not end here. Another phenomenon called thermal turbulence hindered our results as well. It is produced by the changes in the refractive index of air due to the heat of the city. This is in turn, causes fluctuations in the brightness and location of cosmic objects; therefore, blurring them. This is called scintillation, and it reduces the relative optical quality of the atmosphere, known as astronomical seeing. This makes the stars appear as if they are ‘twinkling’. These occurrences are most effective on stars close to the horizon, where the refractive variations are highest. A common example of this is when we see rippled lines of air above a hot asphalt road. [14]

New telescopes and observatories are often built on high mountains above most of the clouds, and in rural areas to counteract the pollution. Some are even placed on islands, because the surrounding sea makes the atmosphere more stable, causing less ‘twinkling’.

4.2 Messier 42

Even though our image of Messier 42 in Figure 8b is a high-resolution image, it is no doubt that its quality has been hampered by the constraints described above. Therefore, this image is pale in comparison to the seemingly impossible pictures taken in space, free from earthly restrictions. Our images would be greatly improved by using more powerful equipment and imaging from a place without so many drawbacks.

4.3 Betelgeuse and Bellatrix

It is easy to see the parallels between our data and the online data of *Betelgeuse*; however, we cannot make the most reliable deductions due to two key factors. Firstly, we must remember that we only managed to produce five data points for comparison. This was because we faced the typically unsuitable weather conditions in London at the start of the year. With such a small sample size and no error estimations, it is difficult to definitively indicate an overall trend. Secondly, we calculated an apparent magnitude difference simply from the total pixel brightness of some images. Therefore, it does not represent any accurate scientific data, but merely offers an estimation of the trend of the apparent magnitude.

Putting these restraints aside, there is an obvious resemblance in the trends, as shown by Figure 9. The proximity of the experimental (0.0120) and online (0.0046) gradients of the line of best fits, along with the likeness of the polynomial fits further suggests this claim. Considering the above shortcomings and the potential complications of stargazing in central London, it is reassuring to see these compelling similarities in the results.

During the initial dimming of *Betelgeuse*, there was a lot of speculation as to why it was dimming this drastically, along with a supernova being wrongly predicted. However, this outcome was proven incorrect; following its subsequent brightening to its normal apparent magnitude range (Figure 10). Instead, astronomers came up with two possibilities. Firstly, it could have been due to significant cooling of the stellar surface; however, a recent study showed that the drop in temperature was only 50-100 °C, not enough to warrant this radical darkening.

The second more plausible theory is that a giant dust cloud was shed by the star and ejected towards us. Red giants are known to shed material from their surfaces long before they supernova, which condenses around the star as dust. As the dust cools, it absorbs some of the photons coming towards us, hence blocking our view. Recent infrared images taken by The Very Large Telescope concur with this explanation, showing a layer of dust engulfing *Betelgeuse* and emitting infrared light. Today, scientists continue to carefully examine how *Betelgeuse* is brightening up again, as it could contain some new insight to the life cycle and evolution of red variable supergiants. [15]

4.4 Stellar Spectra

The spectra we generated from the images of the stars are far better representations of scientific data as we were able to correlate our pixel columns with accurate online wavelengths of the different elements. Out of the nine stars we chose, seven of them followed the predictions and expected trends of the spectral lines across the star types, deviating within reason.

Conversely, the noise in the spectra of *Alphard* and *Betelgeuse* could be down to any of the environmental factors, described at the start of the section; however, it is not clear as to why only these two spectra were negatively affected. It could be because they are dimmer, and therefore, harder to see and capture. You can also see that as we move down the stellar types, the spectra worsen. Starting from Procyon, increasing and getting worse till *Betelgeuse*. However, we don't have any scientific proof for this claim. Another potential reason could be that the spectroscope was not handled carefully enough, causing the star to not remain in a constant position throughout the 60 second exposure. A possible improvement to this would be to use the auto tracking software we were unable to utilise more than once.

5 Conclusion

The initial aims of this project were relatively flexible; however, we got extremely fortunate with our timing as it coincided with an unprecedented cosmic event that became the centre of the astronomic community for a short period; the mysterious dimming of *Betelgeuse*. Even though we only managed to get five viewing sessions and most of our data only converged with the initial dimming phase, we produced some promising trends, and our final data point even correlated with the subsequent increase in brightness. We also found closure, as recent studies showed that the probable cause was a giant cloud of gas and dust that was ejected by the star; thereby interfering with the transmission of light.

Despite the poor weather conditions, and the fiddly nature of the auto tracking technology, we were also able to capture some fantastic high-resolution images of Messier 42.

Finally, on the last night of viewings, we decided to image some stars using the spectroscope, hoping to tick all the stellar types. It started off as a long shot, but we ended up with at least one star in each stellar group. Even though two of the spectra had too much noise to identify any spectral lines, we were delighted by the seven out of nine spectra that were clean enough to match the expectations of the different classifications, and had the spectral lines we were hoping to identify.

6 Code

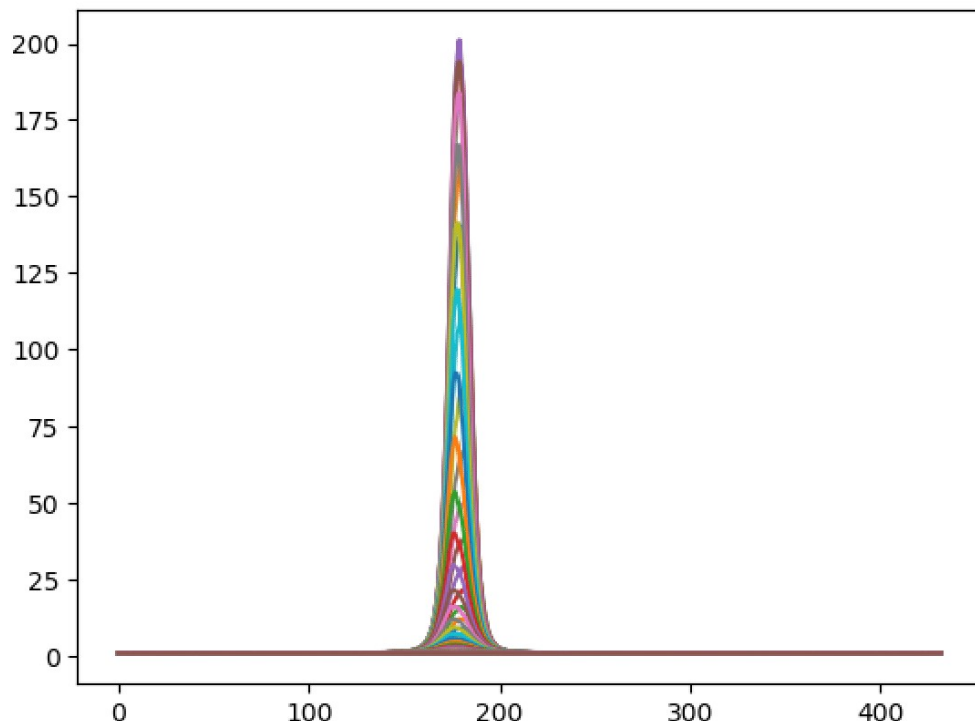
6.1 Sessions 1-5

Relevant parts of the Session 1 code as described in Section 2.4.2.

```
[5]: hdulist2a=fits.open(r"C:\Users\dhruv\Desktop\Project Pics\Betelgeuse\Session 1\betelgeuse_751.fit")
hdulist3a=fits.open(r"C:\Users\dhruv\Desktop\Project Pics\Betelgeuse\Session 1\betelgeuse_752.fit")
hdulist4a=fits.open(r"C:\Users\dhruv\Desktop\Project Pics\Betelgeuse\Session 1\betelgeuse_753.fit")
hdulist5a=fits.open(r"C:\Users\dhruv\Desktop\Project Pics\Betelgeuse\Session 1\betelgeuse_754.fit")
hdulist6a=fits.open(r"C:\Users\dhruv\Desktop\Project Pics\Betelgeuse\Session 1\betelgeuse_755.fit")
hdulist7a=fits.open(r"C:\Users\dhruv\Desktop\Project Pics\Betelgeuse\Session 1\betelgeuse_756.fit")
hdulist8a=fits.open(r"C:\Users\dhruv\Desktop\Project Pics\Betelgeuse\Session 1\betelgeuse_757.fit")
hdulist9a=fits.open(r"C:\Users\dhruv\Desktop\Project Pics\Betelgeuse\Session 1\betelgeuse_758.fit")
hdulist10a=fits.open(r"C:\Users\dhruv\Desktop\Project Pics\Betelgeuse\Session 1\betelgeuse_759.fit")
hdulist11a=fits.open(r"C:\Users\dhruv\Desktop\Project Pics\Betelgeuse\Session 1\betelgeuse_760.fit")
hdulist12a=fits.open(r"C:\Users\dhruv\Desktop\Project Pics\Betelgeuse\Session 1\betelgeuse_761.fit")
hdulist13a=fits.open(r"C:\Users\dhruv\Desktop\Project Pics\Betelgeuse\Session 1\betelgeuse_762.fit")
hdulist14a=fits.open(r"C:\Users\dhruv\Desktop\Project Pics\Betelgeuse\Session 1\betelgeuse_763.fit")

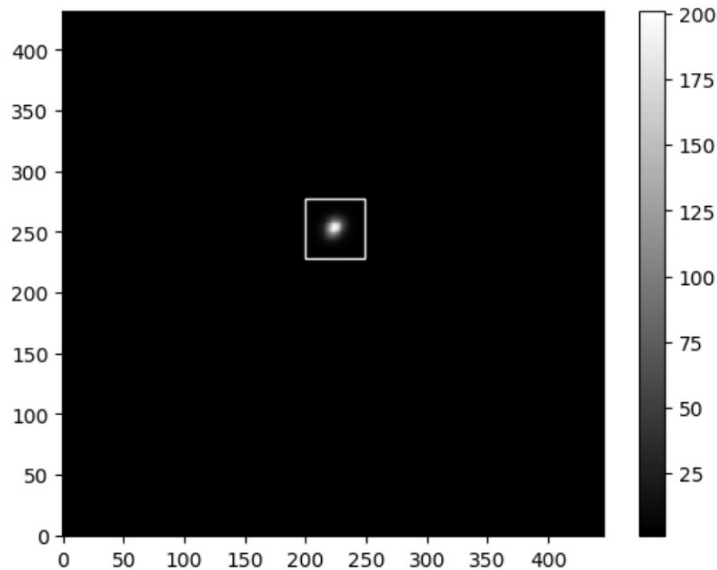
data2a = (hdulist2a[0].data)/256
data3a = (hdulist3a[0].data)/256
data4a = (hdulist4a[0].data)/256
data5a = (hdulist5a[0].data)/256
data6a = (hdulist6a[0].data)/256
data7a = (hdulist7a[0].data)/256
data8a = (hdulist8a[0].data)/256
data9a = (hdulist9a[0].data)/256
data10a = (hdulist10a[0].data)/256
data11a = (hdulist11a[0].data)/256
data12a = (hdulist12a[0].data)/256
data13a = (hdulist13a[0].data)/256
data14a = (hdulist14a[0].data)/256

sum1=data1a+data2a+data3a+data4a+data5a+data6a+data7a+
data8a+data9a+data10a+data11a+data12a+data13a+data14a
average1 = sum1/14
ax1a = plt.plot(average1)
```



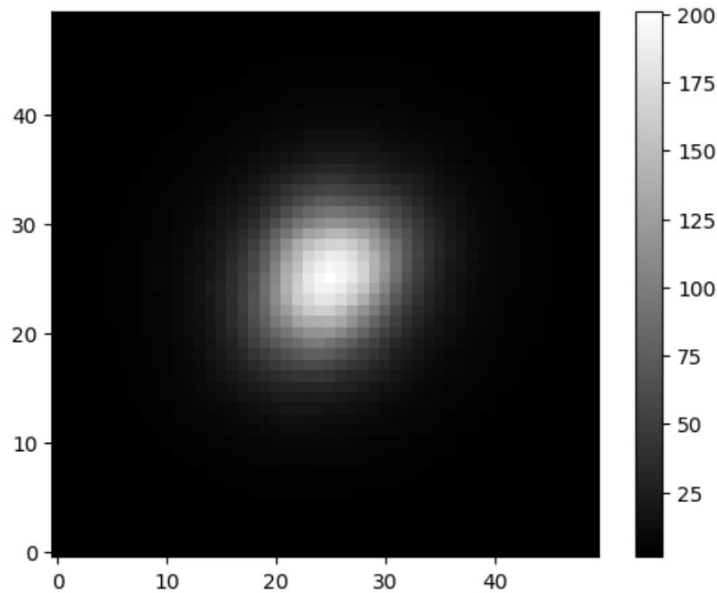
```
[7]: position2 = (224, 253)
      size2 = (50,50)
      cutoutf1 = Cutout2D(np.flipud(average1), position2, size2)
      plt.imshow(np.flipud(average1), origin='lower', cmap='gray')
      cutoutf1.plot_on_original(color='white')
      plt.colorbar()
```

```
[7]: <matplotlib.colorbar.Colorbar at 0x1f0976b1780>
```



```
[8]: plt.imshow(cutoutf1.data, origin='lower', cmap='gray')
      plt.colorbar()
```

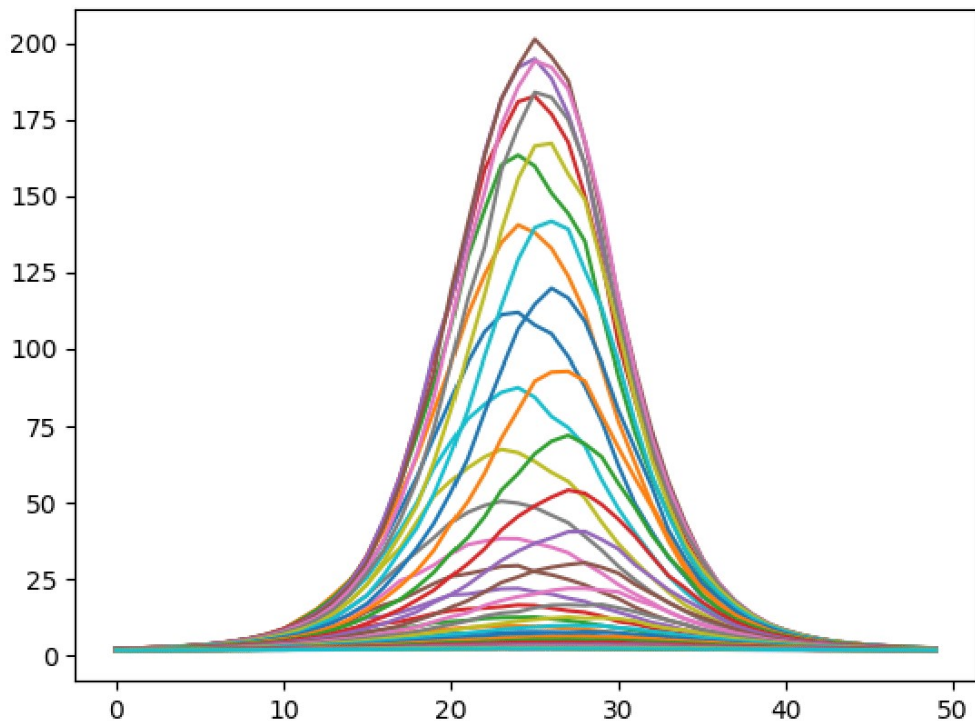
```
[8]: <matplotlib.colorbar.Colorbar at 0x1f098c15d30>
```



```
[9]: xf1 = cutoutf1.data
ax1b = plt.plot(xf1)
b1 = np.sum(xf1)
print(b1)

print('Min:', np.min(xf1))
print('Max:', np.max(xf1))
print('Mean:', np.mean(xf1))
print('Stdev:', np.std(xf1))
```

37790.534877232145
 Min: 1.4037388392857142
 Max: 201.20870535714286
 Mean: 15.116213950892858
 Stdev: 31.45530487585932



This whole code was then repeated for *Bellatrix* as well.

```
[20]: b1, b2
```

```
[20]: (37790.534877232145, 11475.37109375)
```

```
[21]: b1/b2
```

```
[21]: 3.293186300337996
```

```
[22]: a = math.log(b1/b2,2.512)
a
```

```
[22]: 1.29397723187503
```

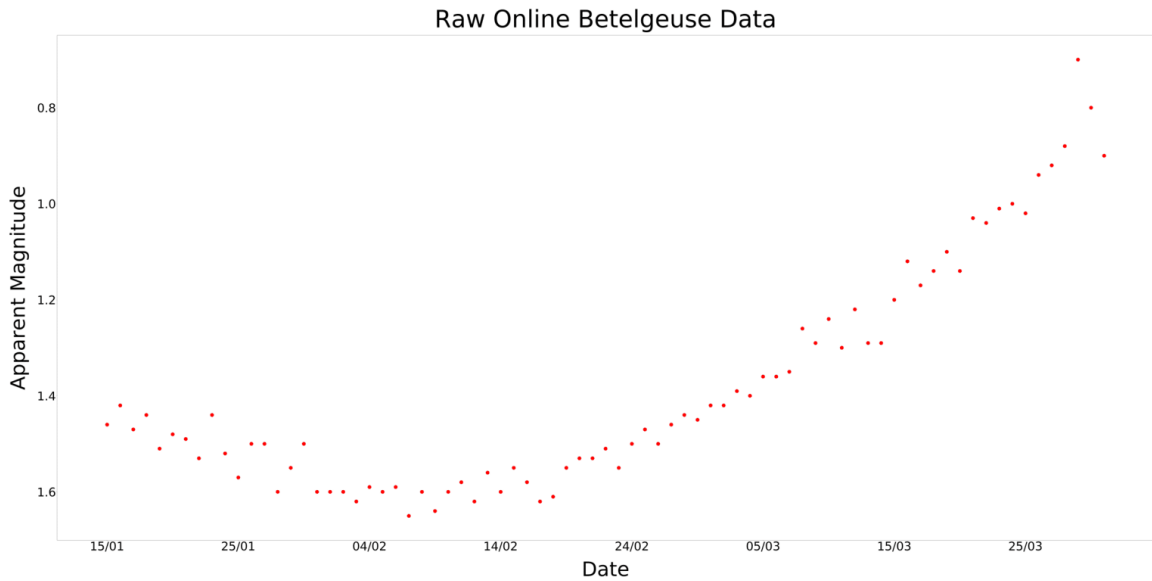
Finally, the brightness ratios (b_1 and b_2) were used to calculate the difference in apparent magnitude (a) for that night. This whole code was modified and run after each of the five sessions to produce the five data points.

6.2 Betelgeuse Tracking

Relevant parts of the *Betelgeuse* tracking code as discussed in Section 3.2.

```
dates=[["15/01", "16/01", "17/01", "18/01", "19/01", "20/01", "21/01", "22/01", "23/01", "24/01", "25/01",
"26/01", "27/01", "28/01", "29/01", "30/01", "31/01", "01/02", "02/02", "03/02", "04/02", "05/02", "06/02",
"07/02", "08/02", "09/02", "10/02", "11/02", "12/02", "13/02", "14/02", "15/02", "16/02", "17/02", "18/02",
"19/02", "20/02", "21/02", "22/02", "23/02", "24/02", "25/02", "26/02", "27/02", "28/02", "29/02", "01/03",
"02/03", "03/03", "04/03", "05/03", "06/03", "07/03", "08/03", "09/03", "10/03", "11/03", "12/03", "13/03",
"14/03", "15/03", "16/03", "17/03", "18/03", "19/03", "20/03", "21/03", "22/03", "23/03", "24/03", "25/03",
"26/03", "27/03", "28/03", "29/03", "30/03", "31/03"]]
values=[[1.46, 1.42, 1.47, 1.44, 1.51, 1.48, 1.49, 1.53, 1.44, 1.52, 1.57, 1.5, 1.5, 1.6, 1.55, 1.5, 1.6, 1.6,
1.6, 1.62, 1.59, 1.6, 1.59, 1.65, 1.6, 1.64, 1.6, 1.58, 1.62, 1.56, 1.6, 1.55, 1.58, 1.62, 1.61, 1.55, 1.53, 1.53,
1.51, 1.55, 1.5, 1.47, 1.5, 1.46, 1.44, 1.45, 1.42, 1.42, 1.39, 1.4, 1.36, 1.36, 1.35, 1.26, 1.29, 1.24, 1.3,
1.22, 1.29, 1.29, 1.2, 1.12, 1.17, 1.14, 1.1, 1.14, 1.03, 1.04, 1.01, 1, 1.02, 0.94, 0.92, 0.88, 0.7, 0.8, 0.9])

matplotlib.rc('xtick', labelsize=75)
matplotlib.rc('ytick', labelsize=75)
plt.figure(figsize=(100,50))
ax = plt.scatter(dates,values,s=500,color="red")
ax=plt.gca()
ax.invert_yaxis()
ax.set_xticks(ax.get_xticks()[:10])
plt.xlabel('Date', fontdict = {'fontsize' : 125},labelpad=50)
plt.ylabel('Apparent Magnitude', fontdict = {'fontsize' : 125}, labelpad=50)
plt.title("Raw Online Betelgeuse Data",fontdict = {'fontsize' : 150},pad=50)
plt.tight_layout()
plt.show()
```



```

def findas(m,xs,ys):
    A= array([[0]*(m+1)]*(m+1))
    b= array([0]*(m+1))
    for k in range(m+1):
        b[k]= sum(ys*xs**k)
        for i in range(m+1):
            A[k,i]= sum(xs**(k+i))
    coefs= linalg.solve(A,b)
    def fit(x):
        return sum(coefs*(x**array(range(len(coefs))))))
    return fit

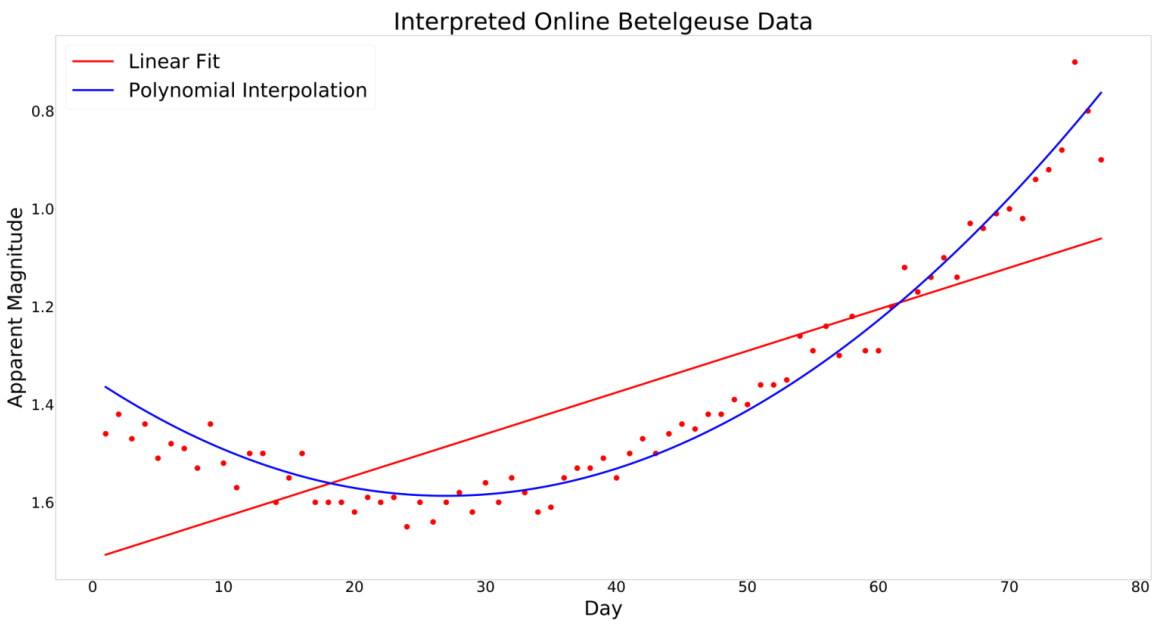
xr = arange(1,len(dates)+1)
yr = values

ftr = findas(2,xr,yr)
xdr = linspace(1,xr.max(),1000)
fitlist = list(map(lambda x: ftr(x),xdr))

matplotlib.rc('xtick', labelsize=75)
matplotlib.rc('ytick', labelsize=75)
plt.figure(figsize=(100,50))
axr = plt.scatter(xr,yr,s=750,color="r")
plt.xlabel('Day', fontdict = {'fontsize' : 100},labelpad=25)
plt.ylabel('Apparent Magnitude', fontdict = {'fontsize' : 100}, labelpad=25)
mr, br = np.polyfit(xr, yr, 1)
plt.plot(xr, mr*xr + br,"r", linewidth=10, label='Linear Fit')
plot(xdr,fitlist,"b", linewidth=10, label='Polynomial Interpolation')
axr=plt.gca()
axr.invert_yaxis()
plt.title("Interpreted Online Betelgeuse Data",fontdict = {'fontsize' : 120},pad=30)

plt.legend(loc=0,fontsize=100)
plt.show()

```



The above parts of the code were updated daily to keep track of *Betelgeuse*'s brightness, up until this report was written. Hopefully, the code continues to be revised in the future, until the star returns to its usual brightness range.

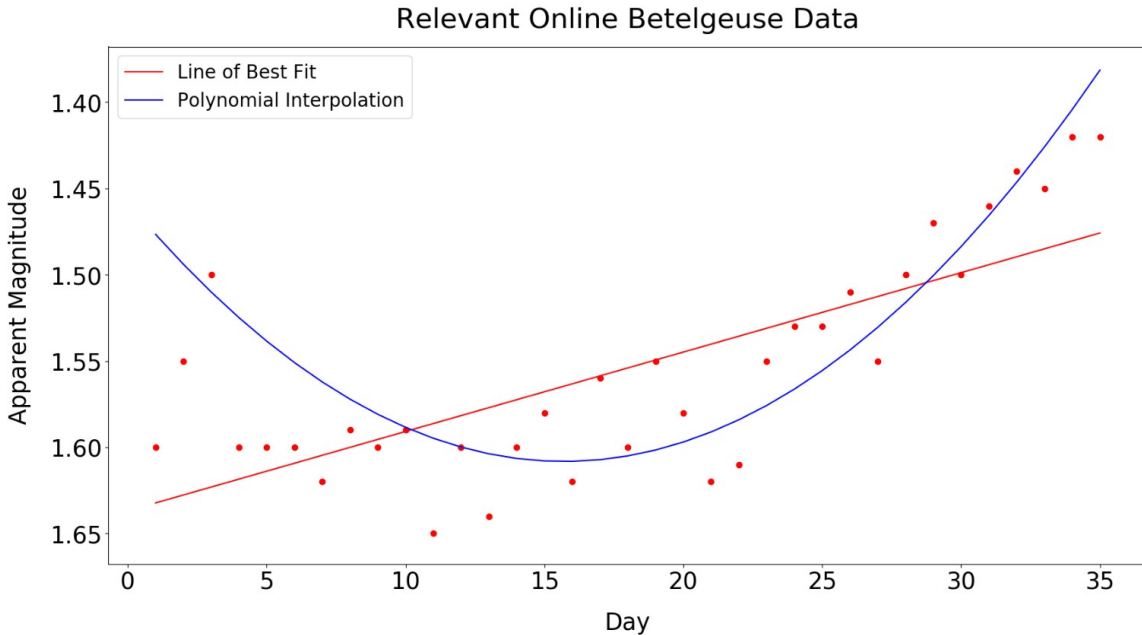
```

x1=arange(1, 36)
y1=[[1.6,1.55,1.5,1.6,1.6,1.6,1.62,1.59,1.6,1.59,1.65,1.6,1.64,1.6,1.58,1.62,1.56,1.6,1.55,
1.58,1.62,1.61,1.55,1.53,1.53,1.51,1.55,1.5,1.47,1.5,1.46,1.44,1.45,1.42,1.42]])

ft1 = findas(2,x1,y1)
xd1 = arange(1,36)
fitlist1 = list(map(lambda x: ft1(x),xd1))

matplotlib.rcParams['xtick', labelsize=25]
matplotlib.rcParams['ytick', labelsize=25]
plt.figure(figsize=(20,10))
m1, b1 = np.polyfit(x1, y1, 1)
ax1 = plt.scatter(x1,y1,color="red")
plt.plot(x1, m1*x1 + b1,"r",label='Line of Best Fit')
plt.xlabel('Day', fontdict = {'fontsize' : 25},labelpad=20)
plt.ylabel('Apparent Magnitude', fontdict = {'fontsize' : 25}, labelpad=20)
plot(xd1,fitlist1,"b",label='Polynomial Interpolation')
ax1=plt.gca()
ax1.invert_yaxis()
plt.title("Relevant Online Betelgeuse Data",fontdict = {'fontsize' : 30},pad=20)
plt.legend(loc=2,fontsize=20)
plt.show()

```



```

C1 = 1.29397723187503
C2 = 1.0939899479916453
C3 = 1.207366525644165
C4 = 0.947509025809569
C5 = 1.7244605845038288

```

This was the cropped version of the online data that was used to compare with our experimental data (C1, C2, C3, C4, C5). This was done to ensure that both times frames coincided for a better interpretation.

```

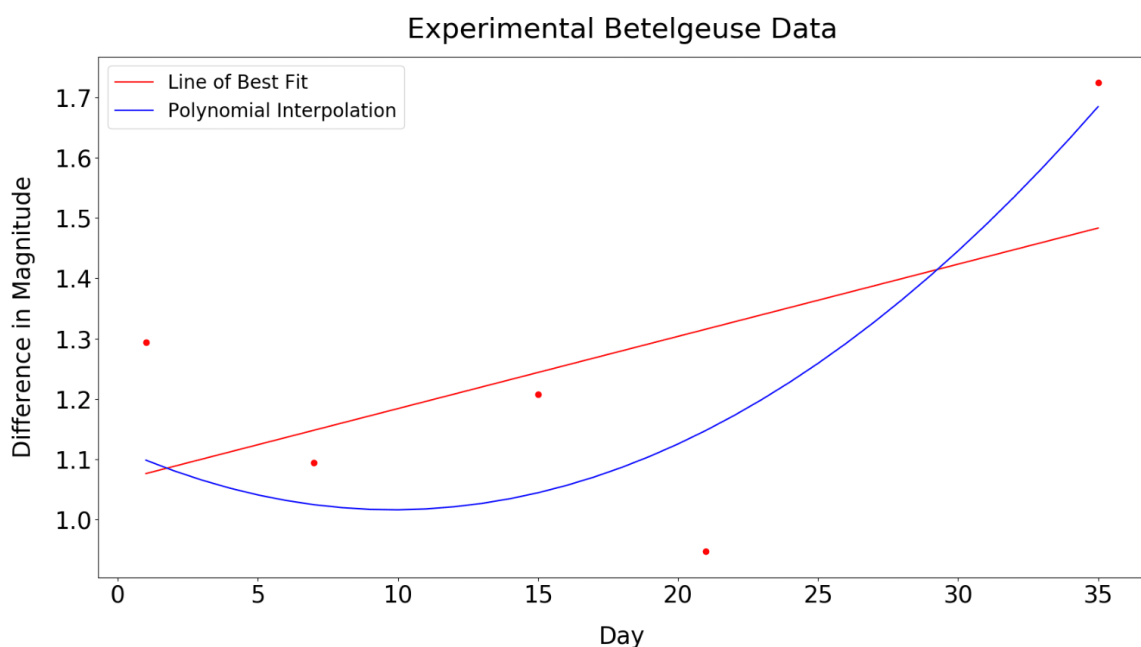
x2 = ([1,7,15,21,35])
y2 = ([C1,C2,C3,C4,C5])

ft2 = findas(2,np.array(x2),y2)

xd2 = arange(1,36)
fitlist2 = list(map(lambda x: ft2(x),xd2))

matplotlib.rc('xtick', labelsize=25)
matplotlib.rc('ytick', labelsize=25)
plt.figure(figsize=(20,10))
m2, b2 = np.polyfit(x2, y2, 1)
ax2 = plt.scatter(x2,y2,color="red")
plt.plot(xd2, m2*xd2 + b2, "r",label='Line of Best Fit')
plt.xlabel('Day', fontdict = {'fontsize' : 25},labelpad=20)
plt.ylabel('Difference in Magnitude', fontdict = {'fontsize' : 25}, labelpad=20)
plot(xd2,fitlist2,"b",label='Polynomial Interpolation')
plt.legend(loc=2,fontsize=20)
plt.title("Experimental Betelgeuse Data",fontdict = {'fontsize' : 30},pad=20)
plt.show()

```



```

matplotlib.rc('xtick', labelsize=20)
matplotlib.rc('ytick', labelsize=20)
fig, ax1 = plt.subplots(figsize=(20,10))

color = 'red'
ax1.set_xlabel('Day',fontdict = {'fontsize' : 30},labelpad=20)
ax1.set_ylabel('Apparent Magnitude', color=color,fontdict = {'fontsize' : 30},labelpad=20)
ax1.plot(x1, y1, color=color,label='Online')
ax1 = plt.gca()
ax1.invert_yaxis()
ax1.tick_params(axis='y', labelcolor=color)

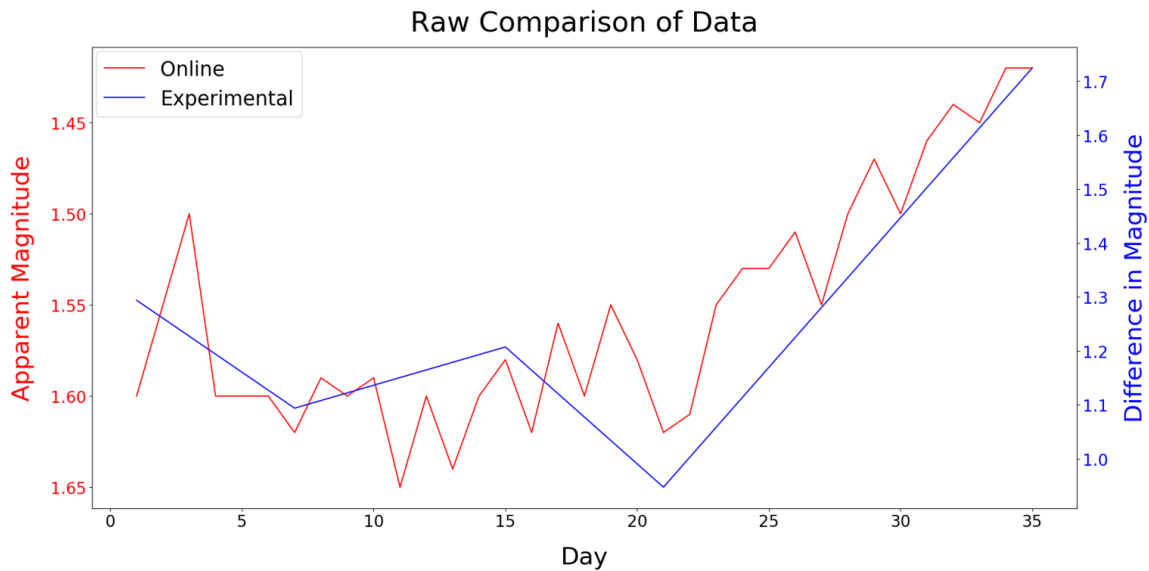
ax2 = ax1.twinx()

color = 'blue'
ax2.set_ylabel('Difference in Magnitude', color=color,fontdict = {'fontsize' : 30},labelpad=20)
ax2.plot(x2, y2, color=color,label='Experimental')
ax2.tick_params(axis='y', labelcolor=color)

fig.legend(loc=2, bbox_to_anchor=(0.07,0.925), fontsize=25)
plt.title("Raw Comparison of Data",fontdict = {'fontsize' : 35},pad=20)

fig.tight_layout()
plt.show()

```



```

matplotlib.rc('xtick', labelsize=20)
matplotlib.rc('ytick', labelsize=20)
fig, ax1 = plt.subplots(figsize=(20,10))

color = 'red'
ax1.set_xlabel('Day',fontdict = {'fontsize' : 30},labelpad=20)
ax1.set_ylabel('Apparent Magnitude', color=color,fontdict = {'fontsize' : 30},labelpad=20)
ax1.tick_params(axis='y', labelcolor=color)
m1, b1 = np.polyfit(x1, y1, 1)
ax1.scatter(x1, y1, color=color,label='Online')
ax1 = plt.gca()
ax1.invert_yaxis()
plt.plot(x1, m1*x1 + b1,"r")

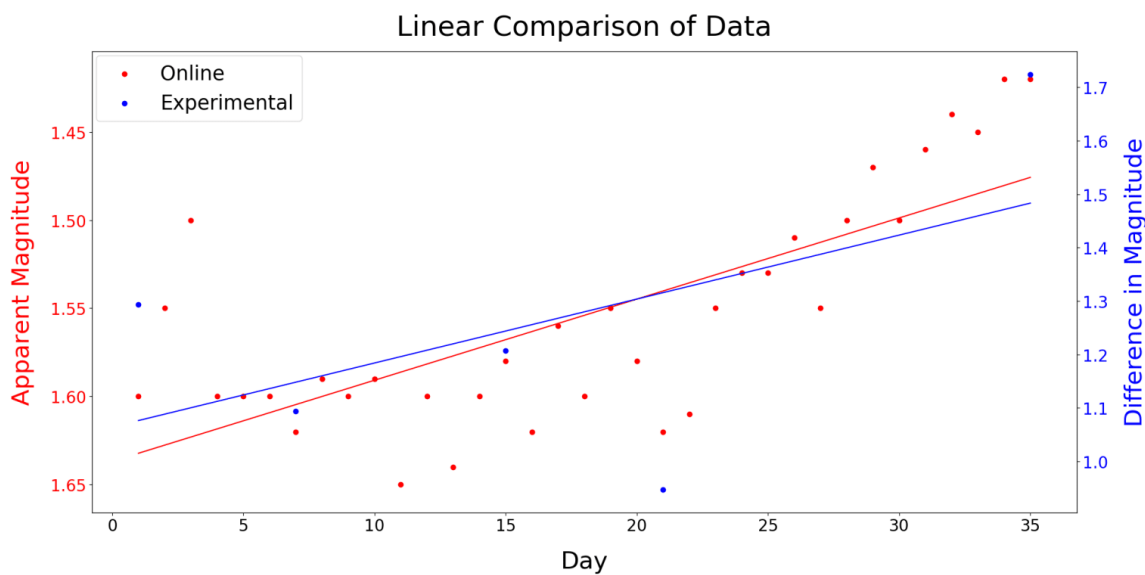
ax2 = ax1.twinx()

color = 'blue'
ax2.set_ylabel('Difference in Magnitude', color=color,fontdict = {'fontsize' : 30},labelpad=20)
ax2.tick_params(axis='y', labelcolor=color)
m2, b2 = np.polyfit(x2, y2, 1)
ax2.scatter(x2, y2, color=color,label='Experimental')
plt.plot(x2, m2*np.array(x2) + b2,"b")

fig.legend(loc=2, bbox_to_anchor=(0.07,0.925), fontsize=25)
plt.title("Linear Comparison of Data",fontdict = {'fontsize' : 35},pad=20)

fig.tight_layout()
plt.show()

```



```

matplotlib.rc('xtick', labelsize=20)
matplotlib.rc('ytick', labelsize=20)
fig, ax1 = plt.subplots(figsize=(20,10))

color = 'red'
ax1.set_xlabel('Day',fontdict = {'fontsize' : 30},labelpad=20)
ax1.set_ylabel('Apparent Magnitude', color=color,fontdict = {'fontsize' : 30},labelpad=20)
ax1.tick_params(axis='y', labelcolor=color)
ax1.scatter(x1, y1, color=color,label='Online')
ax1 = plt.gca()
ax1.invert_yaxis()
plt.plot(xd1,fitlist1,"r")

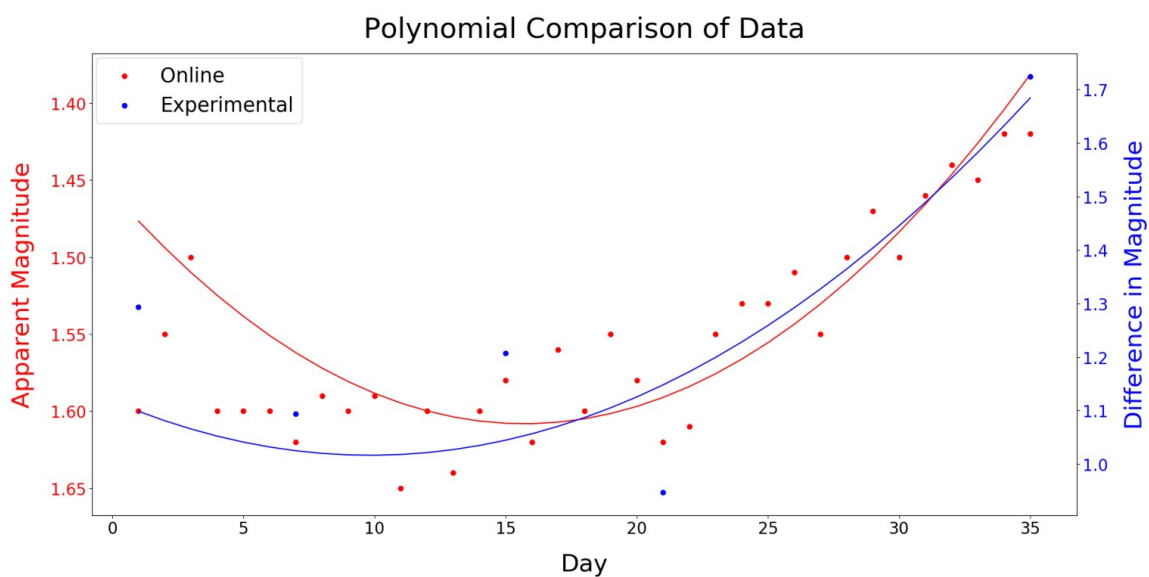
ax2 = ax1.twinx()

color = 'blue'
ax2.set_ylabel('Difference in Magnitude', color=color,fontdict = {'fontsize' : 30},labelpad=20)
ax2.tick_params(axis='y', labelcolor=color)
ax2.scatter(x2, y2, color=color,label='Experimental')
plt.plot(xd2,fitlist2,"b")

fig.legend(loc=2, bbox_to_anchor=(0.07,0.925), fontsize=25)
plt.title("Polynomial Comparison of Data",fontdict = {'fontsize' : 35},pad=20)

fig.tight_layout()
plt.show()

```

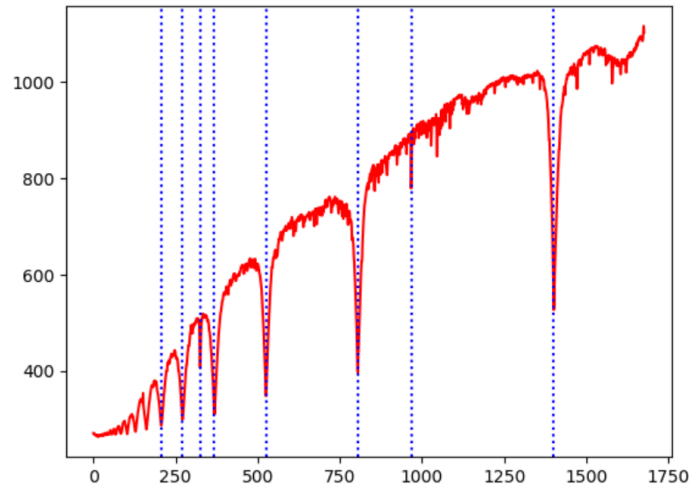


The above code snippets were used to produce the three comparison graphs in Figure 9.

6.3 Stellar Spectra

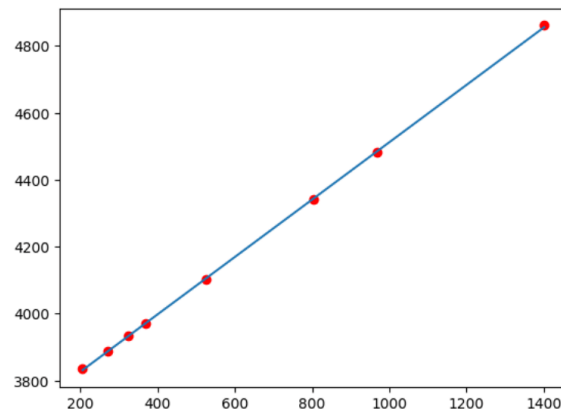
The start of this code was roughly the same as the start of the Session codes, shown in Section 6.1.

```
a = np.mean([a1, a2], axis=0)
plt.plot(a,"r")
plt.axvline(x=206,color='b',ls=":")
plt.axvline(x=271,color='b',ls=":")
plt.axvline(x=325,color='b',ls=":")
plt.axvline(x=368,color='b',ls=":")
plt.axvline(x=525,color='b',ls=":")
plt.axvline(x=805,color='b',ls=":")
plt.axvline(x=967,color='b',ls=":")
plt.axvline(x=1401,color='b',ls=":")
```



```
x1=np.array([206,271,325,368,525,805,967,1401])
y1=np.array([3835.384,3889.049,3933.66,3970.072,4101.74,4340.462,4481.325,4861.3615])
m1, b1 = np.polyfit(x1, y1, 1)
plt.scatter(x1,y1,color="red")
plt.plot(x1,m1*x1+b1)
print(m1)
print(b1)
```

```
0.8577725594184913
3654.6770850938474
```

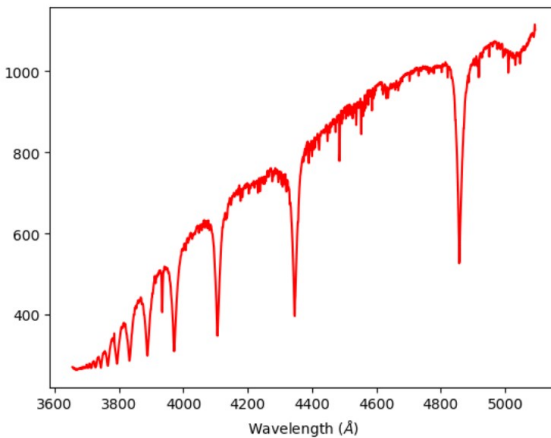


```

xo1 = np.arange(1,1678)
func1 = lambda t: (m1*t)+b1
xn1 = np.array([func1(xi) for xi in xo1])
plt.plot(xn1,a,"r")
plt.xlabel ('Wavelength ($\AA$)')
min(xn1),max(xn1)

```

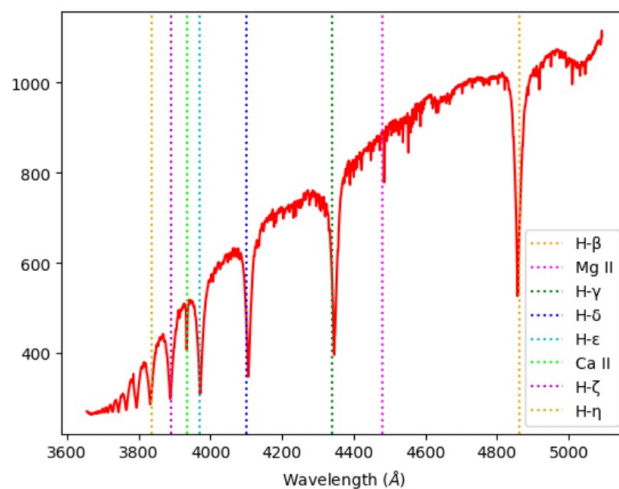
(3655.534857653266, 5093.161667238657)



```

plt.plot(xn1,a,"r")
plt.xlabel ('Wavelength ($\AA$)')
plt.axvline(x=4861.3615,color='orange',label="H-\u03b2",ls=":")
plt.axvline(x=4481.325,color='magenta',label="Mg II",ls=":")
plt.axvline(x=4340.462,color='g',label="H-\u03b3",ls=":")
plt.axvline(x=4101.74,color='b',label="H-\u03b4",ls=":")
plt.axvline(x=3970.072,color='c',label="H-\u03b5",ls=":")
plt.axvline(x=3933.66,color='lime',label="Ca II",ls=":")
plt.axvline(x=3889.049,color='m',label="H-\u03b6",ls=":")
plt.axvline(x=3835.384,color='y',label="H-\u03b7",ls=":")
plt.legend()

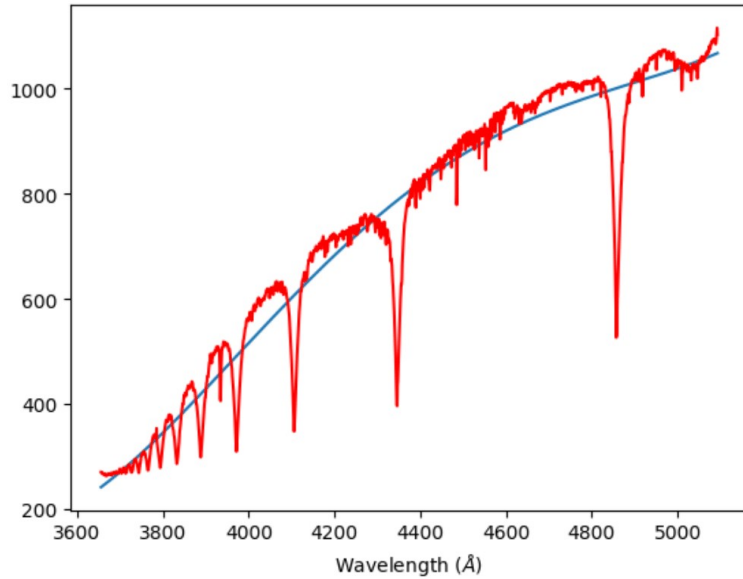
```



```

coefs1 = poly.polyfit(xn1, a, 4)
ffit1 = poly.Polynomial(coefs1)
plt.plot(xn1, ffit1(xn1))
plt.plot(xn1,a,"r")
plt.xlabel ('Wavelength ($\AA$)')

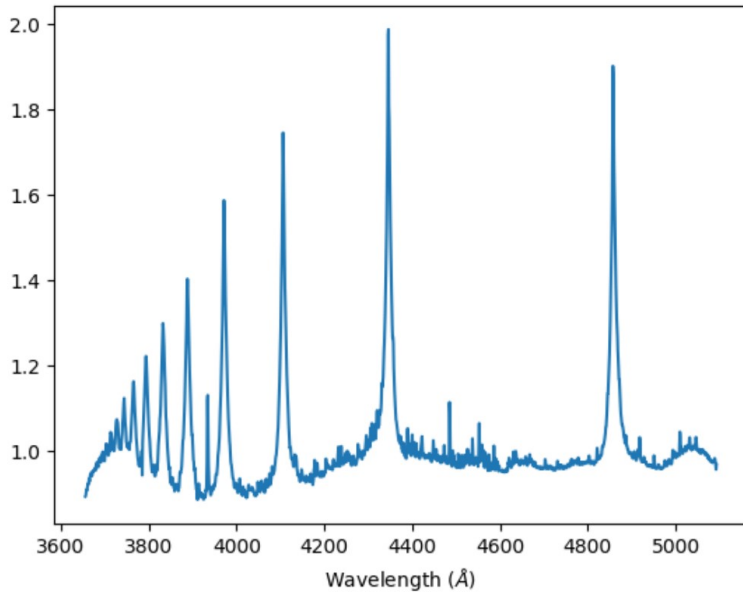
```



```

plt.plot(xn1,ffit1(xn1)/a)
plt.xlabel ('Wavelength ($\AA$)')

```



This is only the code for the first star, *Alhena*, as described in Section 2.5.2. This whole code was then repeated for all the other stars.

References

- [1] Unsöld Albrecht and Bodo Baschek. In: *The New Cosmos*. Springer, 1991, p. 1.
- [2] Tomoya Hirota, Takeshi Bushimata, and et al. “Distance to Orion KL Measured with VERA”. In: *Publications of the Astronomical Society of Japan* 59.5 (Oct. 2007), pp. 897–903. ISSN: 0004-6264. DOI: 10.1093/pasj/59.5.897. eprint: <https://academic.oup.com/pasj/article-pdf/59/5/897/17450771/pasj59-0897.pdf>. URL: <https://doi.org/10.1093/pasj/59.5.897>.
- [3] Jesse S. Allen. *The Classification of Stellar Spectra*. URL: http://www.star.ucl.ac.uk/~pac/spectral_classification.html.
- [4] *Betelgeuse*. Dec. 2020. URL: <https://www.constellation-guide.com/betelgeuse/>.
- [5] Apr. 1998. URL: <https://www.phys.ksu.edu/personal/wysin/astro/magnitudes.html>.
- [6] Harvey Richer. *Hubble Sees Faintest Stars in a Globular Cluster*. Aug. 2006. URL: <https://hubblesite.org/contents/news-releases/2006/news-2006-37.html>.
- [7] *Enhanced LCG*. URL: <https://www.aavso.org/LCGv2/>.
- [8] *What Will Happen When Betelgeuse Goes Supernova?* Mar. 2019. URL: <https://www.forbes.com/sites/quora/2019/03/12/what-will-happen-when-betelgeuse-goes-supernova/#2dbc3505459e>.
- [9] *Table of Spectral Lines Used in SDSS*. URL: <http://classic.sdss.org/dr6/algorithms/linestable.html>.
- [10] *Measured Hydrogen Spectrum*. URL: <http://hyperphysics.phy-astr.gsu.edu/hbase/Tables/hydspec.html>.
- [11] Paula Benaglia, Guillermo Bosch, and Cristina Cappa. *Massive stars: Fundamental Parameters and Circumstellar Interactions*. Instituto de Astronomía Universidad Nacional Autónoma de México, 2006.
- [12] Glenn Ledrew. “The Real Starry Sky”. In: *Journal of the Royal Astronomical Society of Canada* 95 (Feb. 2001). Provided by the SAO/NASA Astrophysics Data System, p. 32. URL: <https://ui.adsabs.harvard.edu/abs/2001JRASC..95...32L>.
- [13] P. W. Hodge, Nels Laulainen, and R. J. Charlson. “Astronomy and Air Pollution”. In: *Science* 178.4065 (1972), pp. 1123–1135. ISSN: 0036-8075. DOI: 10.1126/science.178.4065.1123. eprint: <https://science.sciencemag.org/content/178/4065/1123.full.pdf>. URL: <https://science.sciencemag.org/content/178/4065/1123>.
- [14] Bruce MacEvoy. *Astronomical Seeing*. Nov. 2013. URL: <https://www.handprint.com/ASTRO/seeing1.html>.
- [15] Chelsea Gohd. *Weird, dimming star Betelgeuse may have a dusty explanation*. Mar. 2020. URL: <https://www.space.com/betelgeuse-star-dimming-just-dust.html>.